

Pseudoprogression versus true progression in glioblastoma patients: A multiapproach literature review. Part 2-Radiological features and metric markers

Caroline Bund, Benjamin Leroy-Freschini, Roland Schott, Helene Cebula, Georges Noel, Clara Le Fevre, Jean-Marc Constans, Isabelle Chambrelant,

Delphine Antoni

▶ To cite this version:

Caroline Bund, Benjamin Leroy-Freschini, Roland Schott, Helene Cebula, Georges Noel, et al.. Pseudoprogression versus true progression in glioblastoma patients: A multiapproach literature review. Part 2-Radiological features and metric markers. Critical Reviews in Oncology/Hematology, 2021, 159, 10.1016/j.critrevonc.2021.103230. hal-03599517

HAL Id: hal-03599517 https://u-picardie.hal.science/hal-03599517

Submitted on 13 Feb 2023 $\,$

HAL is a multi-disciplinary open access archive for the deposit and dissemination of scientific research documents, whether they are published or not. The documents may come from teaching and research institutions in France or abroad, or from public or private research centers. L'archive ouverte pluridisciplinaire **HAL**, est destinée au dépôt et à la diffusion de documents scientifiques de niveau recherche, publiés ou non, émanant des établissements d'enseignement et de recherche français ou étrangers, des laboratoires publics ou privés.



Distributed under a Creative Commons Attribution - NonCommercial 4.0 International License

Pseudoprogression versus true progression in glioblastoma patients: a multiapproach literature review. Part 2 – Radiological features and metric markers.

Clara Le Fèvre¹, MD MSc, Jean-Marc Constans², MD PhD, Isabelle Chambrelant¹, MSc, Delphine Antoni¹, MD MSc, Caroline Bund³, MD MSc, Benjamin Leroy-Freschini³, MD, Roland Schott⁴, MD MSc, Hélène Cebula⁵, MD MSc, Georges Noël^{1*}, MD PhD.

¹ Department of radiotherapy, ICANS, Institut Cancérologie Strasbourg Europe, 17 rue Albert Calmette, 67200 Strasbourg Cedex, France.

² Department of Radiology, Amiens-Picardie University Hospital, 1 rond-point du Professeur Christian Cabrol, 80054 Amiens Cedex 1, France.

³ Department of Nuclear Medicine, ICANS, Institut Cancérologie Strasbourg Europe, 17 rue Albert Calmette, 67200 Strasbourg Cedex, France.

⁴ Departement of medical oncology, ICANS, Institut Cancérologie Strasbourg Europe, 17 rue Albert Calmette, 67200 Strasbourg Cedex, France.

⁵ Departement of Neurosurgery, Hautepierre University Hospital, 1, avenue Molière, 67200 Strasbourg, France *: Corresponding author: Pr Georges NOEL, Department of radiotherapy, ICANS, Institut Cancérologie Strasbourg Europe, 17 rue Albert Calmette, 67200 Strasbourg Cedex, France, +33 368766969, g.noel@icans.eu

Clara Le Fèvre¹, MD MSc: c.lefevre@icans.eu

Jean-Marc Constans², MD PhD: constans.jean-marc@chu-amiens.fr

Isabelle Chambrelant¹MSc: i.chambrelant@icans.eu

Delphine Antoni¹, MD MSc: d.antoni@icans.eu

Caroline Bund³, MD MSc: c.bund@icans.eu

Benjamin Leroy-Freschini³, MD: b.leroy-freschini@icans.eu

Roland Schott⁴, MD MSc: r.schott@icans.eu

Hélène Cebula⁵, MD MSc: helene.cebula@chru-strasbourg.fr

Georges Noël^{1*}, MD PhD: g.noel@icans.eu

Pseudoprogression versus true progression in glioblastoma patients: a multiapproach literature review.

Part 2 – Radiological features and metric markers.

Highlights

- Patients treated for glioblastoma can experience pseudoprogression
- Differentiating pseudoprogression and true progression is challenging
- A review of predictive imaging markers of pseudoprogression was performed
- Conventional MRI, advanced MRI, spectroscopy and PET features were analyzed

Abstract

After chemoradiotherapy for glioblastoma, pseudoprogression can occur and must be distinguished from true progression to correctly manage glioblastoma treatment and followup. Conventional treatment response assessment is evaluated via conventional MRI (contrastenhanced T1-weighted and T2/FLAIR), which is unreliable. The emergence of advanced MRI techniques, MR spectroscopy, and PET tracers has improved pseudoprogression diagnostic accuracy. This review presents a literature review of the different imaging techniques and potential imaging biomarkers to differentiate pseudoprogression from true progression.

Key words

Diffusion MRI, Glioblastoma, MRS, Perfusion MRI, PET tracers, Pseudoprogression, Progression 1

1. Introduction

2 The estimated number of new brain and nervous system cancer cases in the United States in 3 2020 was 23 890, and there were 18 020 estimated deaths in the same year [1]. Glioblastoma 4 multiforme (GBM), the most common malignant brain primary tumor in adults, represents 5 approximately 60% of all gliomas [2–4]. The incidence of GBM is 3/100,000 in Europe and 6 North America (12 000 patients per year) [5–7]. One-third of patients with GBM survive 1 7 year, with a median survival of 15 to 18 months, and the survival rate is less than 5% at 5 8 years [2,3,8–11], even with improvements in chemoradiotherapy (CRT) [8,12,13]. In a 9 systematic review, the authors established that the 10-year survival rate was 0.71% [14]. 10 Since the introduction of CRT and adjuvant temozolomide (TMZ) following surgery, more 11 patients with GBM have experienced pseudoprogression (PsP) [15–17]than those receiving 12 radiotherapy (RT) alone [8]. PsP is usually a subacute effect that occurs in the first six months 13 after CRT [18-28]. Its mimics progression that evokes response to treatment rather than 14 treatment failure [19,25,29,30]. Its incidence remains variable; the literature reports rates from 15 2% to more than 50%, with a rate of 36% in a recent meta-analysis [31]. During magnetic 16 resonance imaging (MRI) follow-up of patients treated with surgery, CRT and adjuvant TMZ 17 for GBM, suspected images of progression can occur at the site of previously treated GBM or 18 at distant sites. Progression is suspected when conventional MRI shows new or enlarged 19 contrast-enhancing imaging compared to presurgery, postsurgery, or pre-RT MRI [18]. To 20 differentiate between PsP and true progression (TP), MRI is often repeated 4 to 8 weeks after 21 the MRI showing progression in the absence of pathological proof [32]. However, the images 22 per se are not specific to PsP or TP.

Some groups have proposed criteria to guide response assessment to treatment, but those criteria have limits [33–37]. The Macdonald criteria were the first to measure radiological response through the two-dimensional measurement of contrast enhancement [35]. In 2010,

1 the RANO criteria took into account T2/FLAIR signal changes in addition to contrast 2D 2 enhancement measurements [34]. Modified criteria were published for immune therapies and 3 other clinical situations [33,37]. No single imaging feature or combination of features have 4 been validated to date to differentiate PsP and TP [38]. New therapeutics that impact MRI 5 further complicate PsP diagnosis. Moreover, contrast-enhanced image signal MRI is 6 dependent on the contrast dose, injection timing, magnetic field strength, and choice of image 7 sequences [32]. Conventional MRI is limited in response assessment and disease progression 8 monitoring. Some authors proposed evaluation of advanced imaging, now routinely available, 9 to find noninvasive imaging markers, improve PsP diagnosis, and improve patient outcome 10 [39,40]. In addition to supplying structural and anatomical information, advanced MRI 11 provides cellular, biological, and metabolic information [41]. A meta-analysis including 941 12 patients with GBM showed that advanced MRI techniques had higher diagnostic accuracy 13 than conventional MRI for the distinction of PsP and TP, with a sensitivity and specificity of 14 71-92% and 85-95% vs 68% and 77%, respectively. Magnetic resonance spectroscopy (MRS) 15 had the best accuracy with a sensitivity and specificity of 91% and 95%, respectively, 16 followed by perfusion MRI with dynamic contrast-enhanced MRI (DCE) [42]. The authors 17 developed a model-based metric of therapy response based on T1 contrast-enhanced MRI and 18 used linear, 4D-spherical, and 4D-anatomic models to distinguish PsP from TP with a 19 sensitivity of 79%, a specificity of 59%, a positive predictive value (PPV) of 50%, and a 20 negative predictive value (NPV) of 93% [43]. The combination of advanced modalities in 21 multiparametric imaging improves accuracy but requires training, clinical trial data, and 22 standardization.

23 The aim of this analytic review was to discuss the metrics of diffusion MRI, perfusion MRI,

24 MRS, and positron emission tomography (PET) techniques to distinguish PsP from TP.

25 **2.** Methods

A literature search was conducted using the Medline/PubMed, ScienceDirect, and Cochrane 1 Wiley databases. The search terms used included ("glioblastoma" OR "gliomas" OR "high 2 3 grade gliomas") AND ("pseudoprogression" OR "pseudo-progression"). Articles concerning 4 PsP in adult patients treated for glioma, high-grade glioma (HGG) and glioblastoma treated 5 with the Stupp protocol were examined. References provided from relevant articles were also 6 examined to identify additional studies for inclusion. Any irrelevant entries and non-English articles were excluded. A total of 23 articles about conventional MRI, 43 about diffusion 7 8 MRI, 58 about perfusion MRI, 25 about MRS, 59 about PET scan, and 14 about SPECT were 9 included in this review.

10

3. Conventional MRI

11 Conventional gadolinium contrast-enhanced MRI is the gold standard for the measurement of 12 response to treatment but is not efficient in distinguishing TP from PsP [29]. Conventionally, 13 PsP MR images show vasogenic edema due to increased vascular permeability and increased 14 contrast enhancement [19,44]. Santra et al. included 90 patients (16 of whom had GBM) and 15 concluded that the overall sensitivity, specificity, PPV, NPV and accuracy of conventional 16 MRI to detect TP were 83%, 25%, 77%, 33%, and 67%, respectively [45]. For the follow-up 17 of GBM patients treated with CRT, the National Comprehensive Cancer Network (NCCN) 18 suggests 1) preoperative MRI, 2) intraoperative MRI for optimal tumor resection (when 19 available), 3) 48-72 h postoperative MRI, 4) 4-week post-CRT MRI, and 5) repeat MRI every 20 2-4 months according to the disease status and clinical course [46]. To assist clinicians in PsP 21 diagnosis and uniform practices, the International Standardized Brain Tumor Imaging Protocol (BTIP) established the minimum image acquisition requirements for 1.5T and 3T 22 23 MR scans: sagittal/axial T1, axial FLAIR and axial DWI prior to contrast administration, and 24 axial T2 and sagittal/axial T1 after contrast administration [36].

25 **3.1.T1-weighted contrast-enhanced images**

1 Some studies reported that the size of enhancing lesions was higher in TP than in PsP [47,48]. Several TP radiological markers were identified to indicate the involvement of the corpus 2 3 callosum, including either multiple enhancing foci crossing the midline and multiple 4 enhancing lesions or subependymal spread and multiple enhancing lesions [49], 5 subependymal enhancement [50,51], spreading wave front of enhancement [51], the 6 enhancing lesion crossing the midline [47], and solid enhancement with distinct margins and 7 focally enhancing nodules [52]. Hansen et al., in a study including 15 GBM patients with 8 40% unmethylated MGMT promotors and 67% IDH1 wild-type, showed that in 3D MRI, a 9 more spherical, more symmetric and fuller contrast enhancement with reduced perforations in 10 the outer shell of the enhanced region was conducted for TP diagnosis [53]. However, some 11 studies showed that the increase in T1 contrast enhancement was not statistically significant 12 between PsP and TP [20], and the change in the size of the enhancing lesion between baseline MRI and MRI at progression was not a determinant criterion between PsP and TP [47]. In the 13 14 Agarwal et al. study including 46 HGGs, no difference was found in the location of the 15 recurrent volume between PsP and TP [47]. Moreover, no correlation between MRI changes 16 and radiation dose distribution was demonstrated between PsP and TP [47]. The authors 17 showed that the sharp demarcation was poorly defined in PsP compared to TP [47]. Young et 18 al. analyzed 93 GBM patients and demonstrated that new enhancement, marginal 19 enhancement, nodular enhancement, callosal enhancement, a spreading wave front of 20 enhancement, cystic or necrotic changes, increased peritumoral intensity, subsequent 21 decreased enhancement, and diffusion restrictions were not predictive factors of PsP [50]. 22 Textural feature analysis of conventional MRI could help differentiate PsP and TP [54]. 23 The interpretation of T1-weighted enhanced MR images can be prudent because they may be

25 MGMT promoter methylation [15]. Moreover, differential nontumoral diagnoses of

influenced by radiological techniques, corticosteroid use [55], antiangiogenic agents [56] or

enhancing lesions can be performed, such as inflammation, seizure, postsurgical changes, and
 ischemia.

3 **3.2.T2/FLAIR**

A trend toward an increase in FLAIR signal intensity in TP [47,57] was discussed [20]. Some
authors showed an increase in the FLAIR volume favoring TP [58] as the bidimensional size
measurement increased [47]. Moreover, the FLAIR volume in the 45 Gy (75%) isodose
favored PsP [58].

8 The T2/FLAIR signal must be interpreted with caution because it can be influenced by 9 treatment effects, corticosteroids, demyelination, infection, or seizure [34].

10 Due to the similarities between PsP and TP on conventional MRI and the difficulties faced by 11 clinicians and neuroradiologists, advanced imaging techniques, such as MRS, diffusion-12 weighted MRI (DWI), MR perfusion imaging, diffusion-tensor imaging and PET-based 13 strategies, are necessary [59,60]. Multiple sequences were developed to allow several metric 14 measurements, and they are described in Table 1.

15

4. Diffusion-weighted MRI (DWI) and Diffusion tensor imaging (DTI)

16 Advanced MRI techniques can provide additional information when conventional MRI is 17 ambiguous to improve the distinction between PsP and TP [39,61]. Different diffusion 18 modalities and metrics were developed (Table 1) [30,62,63]. Radiation injury images usually 19 show heterogeneity on DWI images and often include spotty and marked hypointensity [64]. 20 Analyzing signal intensity patterns on DWI, Lee et al. showed, in a study enrolling 22 HGG 21 patients (10 with TP, including six that were MGMT promotor methylated, and 12 with PsP, 22 including five that were MGMT promotor methylated), that patients with TP had a higher 23 incidence of homogeneous or multifocal high signal intensity than those with PsP who had rim high or no high intensity signal (p=0.027). The PsP volume was higher than the TP 24 volume (p=0.009) [65]. Xu et al. concluded, in a study of 35 patients, that DTI offered a 25

sensitivity, specificity, PPV, and NPV of 85%, 87%, 89%, and 81%, respectively. The lesion
 classification accuracy was 86% [66].

3

4.1. Apparent Diffusion Coefficient (ADC)

4 ADC helps to distinguish whether enhancing lesions result from TP with the hypothesis that 5 recurrent tumors have low ADC values [30,44,64,67-72]. Van Dijken et al., in a meta-6 analysis of 35 studies and 1174 patients, retrieved an ADC pooled sensitivity and specificity 7 of 71% and 87%, respectively, to differentiate PsP and TP [42]. Some authors reported that 8 ADC values and ADC ratios were higher in PsP patients than in TP patients [64,66,67,73–80], 9 but others did not demonstrate a difference [47,68,81] (Table 2). Al Sayyari et al. used 10 susceptibility-weighted imaging (SWI), which is useful in visualizing heterogeneous tissue 11 patterns; providing information on microvascularity, necrosis, and the blood-brain barrier; and 12 evaluating ADC values in the context of an abnormal blood-brain barrier. The authors 13 compared contrast-enhanced T1-weighted imaging (CE-T1) and contrast-enhanced susceptibility-weighted imaging (CE-SWI) of 17 patients with new contrast enhancement 14 15 after CRT and created ADC maps. They reported that the CE-SWI volume was reduced 16 compared to CE-T1 volume (p=0.002), with no difference in the median ADC value. An 17 increase in CE-SWI volume was associated with a trend toward reduced ADC in TP. Patients 18 with TP had significantly reduced ADC values vs patients with PsP who had significantly 19 elevated ADC values within the CE-SWI enhancement volume [82]. The fifth percentile of 20 ADC maps could be helpful for distinguishing PsP and TP. Song et al. proposed a threshold value of the fifth percentile of 0.892×10^{-3} mm²/s to differentiate PsP and TP with a 21 22 sensitivity of 90% and a specificity of 90% in a study including 20 GBM patients with 70% 23 methylated MGMT promotors (10 each in the TP and PsP groups) [83]. Chu et al. analyzed 24 histograms of ADC maps in 30 GBM patients, of whom 15 were methylated in both the TP 25 and PsP groups and 40% were methylated in the MGMT promoter. The fifth percentile was significantly lower in TP than in PsP regardless of standard or high b value (p=0.049 and
p<0.001, respectively). The authors concluded that the fifth percentile of the cumulative ADC
histogram was a promising parameter with an accuracy of 89% for high b values (b3000) and
67% for standard b values (b1000) [84].

5

4.2.Fractional Anisotropy (FA)

The FA value was higher in TP than in PsP in some studies [66,78,85], but some authors reported no difference [47,68]. Alexiou *et al.* proposed an FA ratio cutoff value of >0.47 for TP with 57% sensitivity and 100% specificity in a study that included 30 HGG patients [78]. In Xu *et al.*'s study, TP was suggested when either an ADC ratio <1.65 or/and an FA ratio >0.36 was detected in the contrast-enhancing lesion [66]. Wang *et al.* showed that an FA threshold value of >0.13 to diagnose TP had a sensitivity of 71% and a specificity of 75% in 41 GBM patients [85].

13 The sensitivity of diffusion MRI was probably sufficient to differentiate PsP and TP, but the 14 specificity remained low [44]. Larger studies with more sophisticated and especially precise 15 analytical techniques are required to determine uniform diffusion parameters.

16

5. Perfusion imaging findings

In a recent European survey, perfusion MRI (table 1) seemed to be used most frequently to
differentiate TP and radiation effects [86]. Optimal thresholds must be determined and
validated prospectively to confirm that the accuracy is sufficient for clinical use.

20

5.1.Dynamic susceptibility contrast MRI (DSC)

DSC is the most used perfusion modality. An inherent limitation of DSC is underestimation of the blood volume in areas of significant blood-brain barrier breakdown [87]. TP is usually characterized by increased blood volume and blood flow secondary to neocapillary formation and dilation of preexisting vasculature, leading to an increase in the relative cerebral blood volume (rCBV) compared to PsP, which is always typified by a decrease in rCBV [88,89]. A meta-analysis investigated 28 studies and 1743 patients and reported that DSC had a sensitivity of 89% and a specificity of 80% to diagnose PsP. With a mean rCBV ranging from 0.9 to 2.15 and a maximum rCBV ranging from 1.49 to 3.1, the sensitivity and specificity to detect TP were 88%/88% and 93%/76%, respectively [90]. Van Dijken *et al.* reported a DSC pooled sensitivity and specificity of 87% and 86%, respectively, to diagnose TP [42].

6 In some studies, rCBV was significantly higher in TP than in PsP [28,75–78,81,85,91–102], 7 but a few studies demonstrated no difference [20,83,103-105](Table 3). Mangla et al. 8 showed, in 36 GBM patients, PsPs and TPs had a mean decrease in rCBV of 41% and 12%, 9 respectively, at one month after CRT [106]. Kong et al. prospectively studied DSC in 59 10 GBM patients with new or enlarged enhancing lesions after CRT and 41% MGMT promoter 11 methylation. A significant difference was observed in rCBV between PsP (0.87) and TP (3.25) for patients with an unmethylated O⁶-methylguanine-DNA methyltransferase (MGMT) 12 13 promoter (p=0.009), while no significant difference was found between rCBV in PsP and 14 rCBV in TP for patients with MGMT promoter methylation (1.56 vs 2.34, p=0.258) [107]. 15 Analyzing changes in kurtosis and skewness derived from normalized rCBV between the first 16 and second post-CRT follow-up of 79 patients with GBM as an imaging biomarker predictor 17 for early treatment response to CRT, Baek et al. demonstrated that histogram parameters 18 (maximum, mode, range, percent change of skewness and kurtosis, and histographic patterns) 19 showed significant differences between PsP and TP. In multivariate analysis, maximum and 20 histographic patterns were independent predictors of TP. Histogram analysis of rCBV can 21 help to differentiate PsP from TP with a sensitivity of 85.7% and a specificity of 89.2% [108]. 22 rPH and PSR were found to be significantly higher and lower, respectively, in TP patients than in PsP patients [91,100]. However, some authors disputed the difference determined by 23 24 PSR [77].

25 **5.2.Dynamic contrast enhanced MRI (DCE)**

DCE was identified as biomarker of PsP [109]. K^{trans} was significantly higher in TP patients [92,110–112], including V_e [111]and V_p [112], but some studies did not show differences in V_e [92,105,110], V_p [111] or K_{ep} [105,110] (Table 3). However, the evaluation time seemed longer since Shin *et al.* demonstrated, in a study including 31 gliomas in 18 GBM patients, that rCBV and rK^{trans} were significantly higher in the TP group than in the PsP group three months after CRT (p=0.007 and p=0.026, respectively) but not within three months (p=0.511 and p= 0.399, respectively) [105].

8 A meta-analysis by Van Dijken *et al.* reported a DCE pooled sensitivity and specificity of
9 92% and 85%, respectively, to diagnose TP [42].

10

5.3.Arterial spin labeling (ASL)

11 ASL is a less frequently used noninvasive perfusion MRI technique [70,113,114]. ASL can 12 help the distinction between PsP and TP [115]. ASL was an independent predictor of TP 13 (OR=4.73; p= 0.0017) with a sensitivity of 79%, a specificity of 64% and improved 14 diagnostic accuracy (from 76% to 89%) when interpreted qualitatively in conjunction with 15 DSC [113]. A meta-analysis retrieved estimates of ASL pooled sensitivity and specificity 16 varying from 52% to 79% and from 64% to 82%, respectively [42]. ASL had a higher 17 sensitivity than DSC (94% vs 71%) for diagnosing TP [116]. The rCBF was significantly 18 higher in patients with TP than in those with PsP in some studies [92,102] but not in others 19 [28,92], according to the authors (Table 3).

20

5.4.Combination of parameters

Multiparametric imaging was useful in the diagnosis of TP vs PsP [117]. Cha *et al.* examined a multiparametric approach combining DWI and perfusion MRI with rCBV and ADC values in 35 patients with GBM (24 with PsP and 11 with TP). Diagnoses based on the multiparametric approach were more accurate than those based on the uniparametric approach, with 82% sensitivity and 100% specificity, and rCBV was the best predictor of TP

1 (p<0.001) [88]. Kim et al. performed measurements using two readers in 169 GBM patients (87 with TP and 82 with PsP). They demonstrated that the addition of conventional MRI and 2 3 DWI with either DSC (p<0.001 and p=0.002 for each reader, respectively) or DCE (p<0.001 4 for both readers) improved the prediction of TP. With the combination of conventional MRI, 5 DWI and DSC, the sensitivity and specificity varied from 82% to 84% and from 95% to 96%, 6 respectively. With the combination of conventional MRI, DWI, and DCE, the sensitivity and 7 specificity varied from 91% to 92% and from 84% to 87%, respectively [51]. Combining 8 DSC and DWI, Prager et al. analyzed 68 HGG patients with 39% MGMT promoter 9 methylation and showed that the sensitivity and specificity of predicting TP were 93% and 10 83%, respectively [77]. In a retrospective study, Park et al. analyzed a volume-weighted 11 voxel-based multiparametric clustering (VVMC) method to distinguish PsP and TP in 162 12 GBM patients (108 in the training set and 54 in the test set; 58% PsP) vs single parametric 13 methods (ADC and CBV). In the entire population, VVMC was significantly improved in 14 differentiating TP and PsP compared with any single parameter, with a sensitivity, specificity, 15 and accuracy varying from 87% to 91% for the three parameters [118]. Seeger et al., in a 16 study including 40 HGG patients, demonstrated that the combination of DCE and DCS 17 perfusion techniques led to an increase in sensitivity and accuracy. ASL could improve the 18 accuracy but not the diagnostic performance of the preexisting combination of DCE and DSC. 19 However, the best multiparametric approach was perfusion MRI and MRS, with an accuracy 20 of 90%, a sensitivity of 83%, and a specificity of 100% [92]. Yoon et al. studied DWI, DSC, 21 and DCE parameters in 75 GBM patients presenting with enlarged contrast-enhanced lesions 22 one month after CRT, and 55% had MGMT promoter methylation. In patients with MGMT 23 promoter methylation, the probability of PsP was 96% when the CBV90 value was <4.02 and 24 90% when ADC10 was >0.94. The results suggested that MRI parameters were stronger predictors of PsP when the MGMT promoter was methylated than when it was unmethylated,
 and DSC had the highest accuracy for PsP [119].

3 5.5.Others modalities

4 After CRT, patients treated for GBM are prone to blood-brain barrier disruption, so the rCBV 5 can be underestimated when gadolinium-based contrast agents are used. Ferumoxytol is a 6 very small supramagnetic iron oxide nanoparticle (30 nm) that can be a relevant substitute 7 because of its potential to act as a blood pool agent shortly after injection [24,120]. In 2011, a 8 pilot study showed a difference between ferumoxytol rCBV and gadoteridol rCBV values 9 (p=0.002) in the TP group but not in the PsP group (p=0.9) [98]. In 2013, the same authors 10 reported significantly improved survival in patients with rCBV values ≤ 1.75 (p=0.001) using 11 ferumoxytol as a prognostic biomarker in differentiating TP from PsP and predicting survival 12 in GBM patients who did not require contrast agent leakage correction [121]. Other authors 13 proposed ferumoxytol as a gadolinium contrast mismatch ratio for PsP biomarkers [122].

Ma *et al.* analyzed 32 patients with gliomas and reported the use of 3T using amide proton transfer-weighted (APTW) imaging features for the differentiation between PsP and TP. APTW_{mean} and APTW_{max} signal intensities were higher in the TP group than in the PsP group (2.75% vs 1.56%; p< 0.001 and 3.29% vs 1.95%; p<0.001). The respective APTW_{mean} and APTW_{max} thresholds for predicting TP were 2.42% (sensitivity of 85% and specificity of 100%) and 2.54% (sensitivity of 95% and specificity of 92%) [123].

Tsien *et al.* proposed using parametric response mapping (PRM) in 27 HGG patients. PRM is a voxel-based imaging method applied to perfusion maps to quantify early hemodynamic alterations after treatment. It can measure the difference between serial rCBV maps for each voxel. P PRM_{rCBV} was significantly different between PsP and TP (p<0.001) and could be considered a potential biomarker to distinguish TP from PsP [104]. Perfusion MRI-fractional tumor burden (pMRI-FTB) was correlated most strongly with
 histologic tumor fraction when compared to other metrics and could be a promising TP
 biomarker [96].

4

6. Magnetic Resonance Spectroscopy (MRS)

5 Both PsP and TP may demonstrate neuronal loss or dysfunction (low NAA), abnormal 6 cellular membrane (high Cho), or anaerobic metabolism (high Lac and Lip) [29]. A meta-7 analysis of 18 articles and 455 glioma patients showed that MRS alone had a moderate impact 8 on the diagnosis of TP, and a Cho/Cr ratio threshold ranging from 1.05 to 2.60 had a 9 sensitivity and specificity of 83%, respectively, and a Cho/NAA ratio threshold ranging from 10 0.88 to 1.90 had a sensitivity and specificity of 88% and 86%, respectively. Consequently, the 11 authors recommended the combination of MRS with advanced imaging technologies [124].

12 MRS can be effective in distinguishing PsP and TP [29,125,126]. In the Zeng et al. study of 13 55 HGG patients, MRS correctly classified 85% of patients in both the TP and PsP groups 14 [74]. Table 4 summarizes the literature data concerning metabolite ratios of MRS [68,74– 15 76,79-81,92,93,127-131]. Elias et al. demonstrated the ability of nonnormalized Cho/NAA 16 and NAA/Cr ratios to identify TP with sensitivity, specificity, PPV, and NPV of 86%, 90%, 17 93%, and 82% and 84%, 93%, 70%, and 82%, respectively. The normalized Cho/NAA ratio 18 offered a sensitivity, specificity, PPV, and NPV of 73%, 40%, 65%, and 50%, respectively, in 19 a study of 27 primary brain tumor patients [132].

Other authors studied the effect of the combination of different imaging modalities to improve PsP identification. Fink *et al.* compared the capacity of multivoxel MRS, single voxel MRS, DSC, and DWI to diagnose TP in 38 glioma patients. The authors suggested that single-voxel MRS was inadequate and that multivoxel MRS should be used to differentiate TP and radiation injuries. The authors proposed a multivoxel Cho/Cr peak area ≥1.54 for a sensitivity, specificity, PPV, NPV, and accuracy of 96%, 83%, 96%, 83%, and 93%, respectively, and a

1 multivoxel Cho/NAA peak height ≥1.05 for a sensitivity, specificity, PPV, NPV, and 2 accuracy of 91%, 83%, 95%, 71%, and 90%, respectively [76]. The conjunction of the 3 metabolite ratios of MRS and ADC of DWI showed that 96% of patients were classified into 4 the correct group. The sensitivity, specificity, and diagnostic accuracy of 3D-MRS were 94%, 5 100% and 96%, respectively [74]. Di Costanzo et al. studied the combination of MRS, 6 conventional MRI, DWI, and perfusion MRI in 29 HGG patients. The discrimination 7 accuracy was 79% when considering only Cho/Cr, 86% when considering Cho/Cr and ADC, 8 90% when considering Cho/Cr and rCBV, and 97% when considering Cho/Cr, ADC, and 9 rCBV [133]. Matsusue et al. demonstrated, in 15 glioma patients, a threshold of 1.30 for the 10 ADC ratio, 2.10 for the rCBV ratio, 1.29 for the Cho/Cr ratio, and 1.06 for the Cho/NAA ratio 11 for accuracies of 87%, 87%, and 85%, respectively. The accuracy of distinguishing TP from 12 PsP reached 93% by combining DWI, DSC, and MRS [134]. A comparison of conventional 13 MRI to MRS, perfusion MRI and FDG-PET in 24 glioma patients (11 GBM) showed that the 14 PPVs were 50%, 92%, 75%, and 100%, respectively. The NPVs for MRS, perfusion MRI, 15 and FDG-PET were 100%, 61%, and 100%, respectively, demonstrating the superiority of 16 MRS and perfusion MRI vs FDG-PET for diagnosing TP [135]. Verma et al. proposed 3D 17 echo-planar spectroscopy to differentiate PsP and TP [136].

Because of user variability to determine the regions of interest and lower spatial resolution, MRS-induced uncertainty, and lack of reproducibility, definition and validation of the thresholds to diagnose PsP and TP is necessary in clinical practice and clinical trials. The limitations of MRS could be the voxel sizes combined with partial volume effects, time acquisition, signal contamination, and the various metabolite ratios used in studies [42,68,74,92,93,133].

24 **7.** Positron-Emission-Tomography (PET)

1 The most common and available PET modality is fluorodeoxyglucose (FDG)-PET, which 2 often has standardized image acquisition but is limited for distinguishing PsP and TP. Novel 3 tracers with lower background brain activity were studied to evaluate TP [137]. Some authors 4 found that amino acid tracers such as methyl-L-methionine (MET), fluoroethyl-L-tyrosine 5 (FET) or fluoro-L-dopa (FDOPA) had higher diagnostic accuracy than conventional and 6 advanced MRI in the differentiation of TP and PsP [6]. The European Association of Nuclear 7 Medicine (EANM), the Society of Nuclear Medicine and Molecular Imaging (SNMMI), the 8 European Association of Neurooncology (EANO), and the Working Group for Response 9 Assessment in Neurooncology with PET (PET-RANO) published guidelines for FDG, MET, 10 FET and FDOPA-PET [138]. The PET images could be matched with contrast-enhanced T1 11 and T2/FLAIR MRI images for interpretation [139-141]. The different PET tracers are 12 summarized in Table 5.

13 Standardization of the methodology and analytical approaches is needed to improve14 comparability and harmonize practices [142].

15 7.1.2-Deoxy-2-[fluorine-18]fluoro-D-glucose positron emission tomography (¹⁸F-FDG 16 PET)

17 Although FDG-PET has already been validated to distinguish PsP and TP [28,45], it has some 18 limitations in the assessment of TP [27,70,137,143–149]. Similar to GBM progression, which 19 demonstrates increased glucose metabolism, radiation injury can also demonstrate increased 20 FDG uptake [150]. Methods to define a cutoff standardized uptake value (SUV) were 21 unreliable because the relative glucose uptake and FDG-PET varied widely for tumors and 22 were different for the normal brain [150]. Ricci et al. concluded, in a study on 31 primary 23 brain tumor patients, that FDG-PET was not a useful tool for the diagnosis of PsP or TP; a 24 comparison with contralateral white matter provided a sensitivity, specificity, PPV, and NPV for the diagnosis of TP of 86%, 22%, 73% and 50%, respectively, and a comparison with 25

1 contralateral gray matter provided corresponding values of 73%, 56%, 80%, and 46%, 2 respectively [151]. However, Santra et al. demonstrated an overall sensitivity, specificity, 3 PPV, NPV, and accuracy of 50%, 100%, 100%, 40%, and 63%, respectively, for diagnosing 4 TP in a GBM subgroup and concluded that FDG-PET was a highly specific modality for 5 detecting TP [45]. In the Larsen et al. study, which included 19 glioma patients (13 GBM), 6 DCE and FDG-PET obtained 81% concordance in the classification of new contrast-enhanced 7 lesions [28]. When FDG-PET was combined with perfusion MRI, DWI, and MRS, the 8 diagnostic accuracy improved [75].

9 Other novel tracers, such as FDOPA, MET, and FET, can be more useful.

10 **7.2.¹⁸F-fluoro-L-dopa positron emission tomography** (¹⁸F-FDOPA PET)

11 FDOPA-PET was useful for complementing the diagnosis of GBM and evaluation of possible 12 progression and detected recurrence earlier than MRI [152-154]. Chen et al. compared 13 FDOPA-PET and FDG-PET and concluded that the sensitivity of FDOPA-PET was higher 14 than that of FDG-PET for detecting tumors, but the sensitivity was the same with both 15 methods: sensitivity, specificity, accuracy, PPV, and NPV of 96%, 43%, 83%, 85%, and 75% 16 for FDOPA-PET and 61%, 43%, 57%, 78%, and 25% for FDG-PET, respectively. The 17 authors proposed a threshold of tumor uptake to striatum uptake (T/S) and tumor uptake to 18 normal hemispheric tissue uptake (T/N) of >1.0 and >1.3 for a sensitivity and a specificity of 19 96%/100% and 96%/86%, respectively [152]. Hermann et al. showed, in 110 GBM patients, 20 that SUV_{max}, SUV_{mean}, T/N_{max}, T/N_{mean}, T/S_{max}, and T/S_{mean} were significantly higher in GBM 21 patients with TP vs no progression, and the T/S_{max} \geq 1.0 threshold had a sensitivity of 84%, a 22 specificity of 62%, and an accuracy of 78% [155]. In another study of 28 glioma patients, the 23 sensitivity, specificity, and accuracy of FDOPA-PET and FDOPA-PET were 48%, 100%, and 24 61% and 100%, 86%, and 96%, respectively, with FDOPA-PET being more sensitive and 25 specific in detecting recurrence [156]. FDOPA-PET and MRI fusion provided anatomical localization precision of abnormal FDOPA-PET activity, and the concordance between both enhancing and nonenhancing lesions on MRI and increased FDOPA-PET uptake was approximately 90%. FDOPA-PET could identify tumors not visible on MRI and was able to distinguish recurrent nonenhancing tumors from other causes of T2 signal changes on MRI [153]. A meta-analysis of 15 articles and 640 patients with primary brain tumors reported that FDOPA-PET was more effective than FET-PET (p=0.015) [157], another amino tracer that was used and studied.

8

7.3.O-(2-[¹⁸F]fluoroethyl) -L-tyrosine positron emission tomography (¹⁸F-FET PET)

9 Several metrics of FET-PET were identified as imaging biomarkers of TP or PsP. In a 10 retrospective study of 22 GBM patients, the mean and maximum tumor-to-brain ratios (TBR_{mean} and TBR_{max}) obtained using FET-PET were higher in the TP group (2.3 and 2.8) 11 12 than in the PsP group (1.8 and 1.9) (p<0.001), and the mean time to peak (TTP) was shorter in the TP group than in the PsP group (p=0.05). The optimal TBR_{max} and TBR_{mean} cutoff values 13 14 for identifying PsP were 2.3 and 2.0, respectively, with a sensitivity of 100% and 82%, a specificity of 91% and 82%, and an accuracy of 96% and 82%, respectively [158]. In another 15 study of 124 glioma patients (50 GBM), the same authors evaluated static and dynamic FET-16 PET. The TBR_{max}, TBR_{mean}, and TTP thresholds for identifying TP were 2.3, 2.0, and <45 17 18 min with sensitivities of 68%, 74%, and 82%; specificities of 100%, 91%, and 73%; and 19 accuracies of 71%, 75%, and 81%, respectively. The combined analysis of TBR_{max} and 20 TBR_{mean} cut-offs and kinetic patterns had a sensitivity of 93%, a specificity of 73%, and an accuracy of 91%, but the combined TBR_{mean} cutoff and TTP cutoff had the best results with a 21 22 sensitivity of 93%, a specificity of 100%, and an accuracy of 93% [159]. Pauleit et al. demonstrated, in a study of 28 glioma patients, that the TBR ratio was an independent 23 24 significant coefficient for the distinction of tumor progression (p=0.004) and reported that the 25 TBR_{mean} was 2.6 in TP vs 1.2 in peritumoral tissue (p<0.001). The sensitivity and specificity

were 92% and 81%, respectively, with a TBR ratio threshold of 1.6 [160]. Kebir et al. 1 2 analyzed 26 GBM patients, 17 of whom had methylated MGMT promotors and reported that 3 TBR_{max} and TBR_{mean} were significantly higher in TP patients than in PsP patients (2.4 vs 1.5, 4 p=0.003 and 2.1 vs 1.5, p=0.012, respectively) and that TTP was lower in the TP group (25 5 min vs 40 min, p<0.001). A TBR_{max} threshold of 1.9 showed a sensitivity, specificity, and 6 accuracy of 84%, 86%, and 85%, respectively [161]. Mihovilovic et al. proposed a TBR_{max} 7 threshold of 3.52 with an accuracy of 86% for late PsP [162]. The 8 EANM/SNMMI/EANO/RANO groups recommended the use of FET-PET with a TBR_{max} 9 threshold of 2.3 to differentiate early PsP and TP and a TBRmax and TBRmean threshold of 1.9 10 to differentiate late PsP and TP [138].

11 Popperl et al. studied 53 glioma patients (27 GBM) and showed that SUV_{max} was superior in 12 cases of TP, and an SUV_{max} threshold of 2.2 had the best differentiation between TP and 13 treatment-related changes. The SUV_{max}/background (BG) ratio threshold had a discriminatory 14 power of 100%. There was also a correlation between the SUV_{max} value and the tumor grade, 15 with high values for high grades [163]. Mehrkens et al. showed, in a study that included 31 16 gliomas (8 GBM), that the PPV of FET-PET was 84% for identifying TP with an SUV_{max}/BG 17 ratio of >2.0 [164]. In a pilot study of 14 HGGs with 86% MGMT promoter methylation (11 18 GBM), Kebir et al. suggested that textural FET-PET features were more predictive of PsP 19 (p=0.041) than the maximum tumor-to-normal brain ratio (TNR_{max}) at an optimal cutoff of 20 2.1 (p=0.07) with a sensitivity, specificity, PPV, and NPV of 90%, 75%, 90%, and 75% and 21 70%, 100%, 100%, and 57%, respectively [165].

Compared to conventional MRI, FET-PET was significantly more accurate (p<0.01) [166].
The adjunction of FET-PET to MRI significantly improved the identification of TP with a
sensitivity and specificity of 93% and 94%, respectively [160]. The combination of FET-PET
and ADC increased the accuracy from 69% to 89% for the differentiation of TP and PsP [167]

Compared to MET-PET, FET-PET provided a comparable ability to differentiate treatment related changes from TP and to delineate the gross target volume (GTV) of tumors with a
 sensitivity of 91% and specificity of 100% for both tracers [168].

4

7.4.¹¹C-methyl-L-methionine positron emission tomography (¹¹C-MET PET)

5 Many studies have demonstrated the use of MET-PET for the management of gliomas. The 6 sensitivity, specificity, and accuracy for detecting TP with MET-PET were 100%, 60%, and 7 82%, respectively [169]. The intensity of MET uptake is associated with the grade of gliomas, 8 so high uptake is associated with poor survival time, indicating MET uptake is a prognostic 9 factor [70,170]. Several studies reported that mean T/N ratio was significantly higher in TP: 4.0 vs 1.8 [171], 4.3 vs 1.8 [172], 2.18 vs 1.49 (p<0.01) [130], 2.69 vs 1.01 (p=0.06) [173], 10 11 1.89 vs 1.44 (p=0.0079) [174], and 2.38 vs 1.04 [93]. The maximum L/N was 2.62 vs 2.11 12 (p=0.052) [174]. A T/N ratio threshold of 2 had a sensitivity of 86% and specificity of 100% 13 [130], and a T/N ratio cutoff of >1.9 had a sensitivity of 95% and specificity of 89% [173]. The SUV_{max} (2.89 vs 1.49 [93] and 3.19 vs 2.66 (p=0.036) [174]) and SUV_{mean} (2.65 vs 1.28 14 15 [93] and 2.31 vs 1.82 (p=0.017) [174]) were both higher in TP patients, and the SUV_{lesion}/BG 16 ratio was also higher in the TP group (2.79 and 1.53) (p<0.05) [175]. In the Garcia et al. study 17 of 30 HGG patients, the sensitivity and specificity were 90% and 100%, respectively, at an 18 SUV/BG threshold of 2.35 [175]. Kim et al. studied 10 HGG patients (5 GBM) and showed a 19 maximal lesion uptake to maximal contralateral cerebral white matter uptake ratio (L/R_{max}) 20 ratio of 2.64 with a sensitivity and specificity of 75% and 100%, respectively [99]. Terakawa 21 et al. determined that L/Nmean was the most informative index, and an L/Nmean cutoff of 1.58 22 had a sensitivity and specificity of 75% and 75%, respectively [174].

Some authors did not demonstrate the use of MET-PET for the differentiation between TP and treatment-related changes. Analyzing MET uptake in lesions and in four specific regions (around the lesion, in the contralateral frontal lobe, in the contralateral area, and in the

1 contralateral cerebellar cortex), MET-PET failed to differentiate treatment-related changes 2 from TP with no significant differences in quantitative or qualitative assessments [176]. No 3 significant differences were reported between treatment-related changes and TP patients in 4 the T/N_{mean} ratio of 1.31 vs 1.87 [169], L/R_{max} ratio of 2.07 vs 3.33; p=0.257 [99], and 5 SUV_{mean} of 1.81 vs 2.44 [169].

6 Compared to FDG-PET, MET-PET was superior to FDG-PET for the detection of tumor 7 recurrence with a sensitivity, specificity, and accuracy of 96%, 87%, and 94% and 46%, 8 100%, and 58%, respectively [177]. The FDG-PET and MET-PET combination provided the 9 highest accuracy (p=0.003), with an accuracy, sensitivity, and specificity of 83%, 95%, and 10 60%, respectively [178]. With a T/N cutoff of >0.75, FDG had a sensitivity and specificity of 11 81% and 89%, respectively, for identifying recurrence, whereas at a T/N cutoff of >1.9, MET had a sensitivity and specificity of 95% and 89%, respectively, for identifying recurrence 12 13 [173].

14 Compared to advanced MRI, MET-PET was more sensitive for diagnosing TP with a sensitivity, specificity, and accuracy of 95%, 80%, and 90%, respectively, whereas advanced 15 16 MRI was more specific, with a sensitivity, specificity, and accuracy of 84%, 90%, and 86%, 17 respectively [93]. Dandois et al. reported that perfusion MRI and MET PET both assisted in diagnosing TP in 28 HGG patients (14 GBM). Of 33 combined MRI and PET studies, 31 18 19 matched perfectly, and rCBV had equal performance with MET-PET [179]. Another study 20 reported that perfusion MRI with rCBV was superior to both MET-PET and FDG-PET for the 21 differentiation between treatment-related changes and TP [99]. Deuschl et al. studied 50 22 glioma patients and proposed a combined use of MRI and PET with hybrid MET-PET/MRI to 23 differentiate treatment-related changes from TP. The sensitivity, specificity, accuracy, and 24 PPV were 86%, 71%, 82%, and 89% for MRI alone, 97%, 74%, 88%, and 86% for MET-25 PET, and 97%, 93%, 96%, and 97% for MET-PET/MRI, respectively. There was a significant difference between MET-PET/MRI and MRI (p=0.008) but no differences between MET PET and MRI alone (p=0.021) or MET-PET/MRI and MET-PET alone (p=1.000) [180].

3 7.5.3'-deoxy-3'[(18)F]-fluorothymidine positron emission tomography (¹⁸F-FLT 4 PET)

5 According to different studies, FLT can assist with glioma detection and grading 6 characterization because its uptake in the normal brain is low, the image contrast is significant 7 [181], and FLT uptake correlates with the Ki67 index [182–185]. It represents a noninvasive 8 method to potentially predict disease progression and response to therapy in gliomas 9 [186,187]. In Choi et al., FLT uptake was correlated with the Ki67 index (p=0.007), and changes in FLT update were associated with response to therapy [185]. However, FLT uptake 10 11 depended on blood-brain barrier disruption, which impacted its efficiency in clinical 12 applications [188]. Muzi et al. proposed a kinetic analysis of FLT in 12 patients with primary 13 brain tumors that quantified FLT uptake and analyzing blood-brain barrier disruption and 14 retention in tumor tissue as a result of metabolic trapping of FLT nucleotides to separate 15 transport effects from tissue retention. They produced a parametric image map of blood-to-16 tissue transport (Kl) and metabolic flux (KFLT). When the blood-brain barrier broke down, 17 transport dominated FLT uptake, but when the blood brain barrier was intact, transport was 18 limited, and FLT-PET was inefficient. The authors concluded that FLT was not the best tracer 19 for necrosis or nonenhancing lesions [189]. In another study of 19 glioma patients (4 GBM), 20 Kl, KFLT, and phosphorylation (K3) were significantly different between TP and treatment-21 related changes (p<0.0001, p=0.0009, and p=0.0012, respectively) when analyzed using the t-22 test, but when the Wilcoxon test was used, only KFLT and K3 demonstrated significant 23 differences. The authors suggested that FLT-PET was promising for the diagnosis of TP with 24 rigorous dynamic parameters [190].

1 Some authors demonstrated that FLT-PET had no use in the discrimination of PsP vs TP. In the den Hollander et al. study evaluating 28 GBM and two gliosarcomas, no difference in 2 3 SUV_{max} was found between patients with TP and patients with PsP [191]. In a more recent prospective study of 24 GBM patients, the SUV_{max} and T/N ratio did not differ significantly 4 5 between the PsP and TP groups (1.41 vs 1.28, p=0.699, and 4.03 vs 3.59, p=0.699, 6 respectively) [192]. Compared to FDG-PET, FLT-PET was not more reliable than FDG-PET 7 for the distinction between TP and treatment-related changes, with a sensitivity and 8 specificity varying from 73% to 91% and 75% vs from 91% to 100% and 75%, respectively 9 [193].

10 **7.6.Others PET tracers**

Other PET tracers were evaluated in the literature. ¹¹C-choline [194], ¹¹C-methyl-L-11 ¹⁸F-fluoromisonidazole 18 F-12 (MLT) [195], (FMISO) [196.197]. tryptophan 13 fluoromethylcholine (FCho) [198], and 4-borono-2-18F-fluoro-phenylalanine (¹⁸F-FBPA) [199,200]could be useful for the differentiation between PsP and TP, but studies are currently 14 15 too rare to promote their use.

16 **7.7.Single photon-emission computed tomography (SPECT)**

In a meta-analysis of 893 patients with gliomas, SPECT was able to differentiate PsP and TP
with a sensitivity of 89% and a specificity of 87% [201]. Some SPECT tracers were studied in
the literature.

In a retrospective study of 19 HGG patients, thallium 201 (²⁰¹Tl)-SPECT had better sensitivity, specificity, PPV, and NPV than conventional MRI (84%, 100%, 100%, and 57% vs 65%, 75%, 92%, and 33%, respectively) and a higher TP diagnostic accuracy (86% vs 67%) [202]. Caresia *et al.* found that the sensitivity, specificity, and accuracy of ²⁰¹Tl-SPECT were 100% [203]. Vos *et al.* estimated that the sensitivity and specificity of ²⁰¹Tl-SPECT ranged from 43% to 100% and from 25% to 100%, respectively. However, the poor

methodological quality and small sample sizes of the included studies impeded conclusions
[204]. Compared to FDG-PET, ²⁰¹Tl-SPECT had a higher sensitivity but a lower specificity
and was better at excluding TP [205].

Sestamibi technetium 99m (^{99m}Tc-MIBI) SPECT had a sensitivity, specificity, and accuracy
of 89%, 83%, and 87%, respectively, for diagnosing TP [206]. Compared with MRS, ^{99m}TcMIBI-SPECT had a sensitivity, specificity, accuracy, PPV, and NPV of 90%, 100%, 93%,
100%, and 83%, respectively, and the combination of ^{99m}Tc-MIBI-SPECT and MRS had a
sensitivity, specificity, accuracy, PPV, and NPV of 95%, 100%, 97%, 100%, and 91%,
respectively [207].

Plotkin *et al.* investigated 123-iodine-a-methyl tyrosine (¹²³I-IMT) SPECT and single voxel MRS in 25 glioma patients (10 GBM) and reported that although ¹²³I-IMT SPECT had a trend of better performance than single voxel MRS, no significant differences were observed in the accuracy, sensitivity, and specificity between the two modalities (p>0.05) for diagnosing TP [131].

Amin *et al.* compared technetium-99m-dimercaptosuccinic acid (^{99m}Tc(V)DMSA)-SPECT and MRS in 24 patients with primary brain tumors (7 GBM) treated with surgery and RCT and concluded that ^{99m}Tc(V)DMSA-SPECT was more effective than MRS for diagnosing TP with a sensitivity, specificity, accuracy, PPV, and NPV of 89%, 100%, 92%, 75%, and 100%, respectively [208].

In 2007, Alexiou *et al.* studied ^{99m}Tc-tetrofosmin (^{99m}Tc-TF) SPECT in 11 patients with glioma (4 GBM) and proposed a lesion uptake to normal brain tissue uptake ratio (L/N) threshold value of 4.76 for diagnosing TP [209]. In 2014, the same authors compared DTI, DSC, and ^{99m}Tc-TF-SPECT in a prospective study of 30 HGG patients and reported an L/N threshold value of 4 with 100% sensitivity and 100% specificity [78]. A comparison of ^{99m}Tc-methionine-SPECT, FDG-PET, and conventional MRI demonstrated that the specificity of ^{99m}Tc-MET-SPECT was significantly higher than the specificity of conventional MRI (p<0.0001) but not the specificity of FDG-PET (p=0.36). No significant difference in sensitivity or accuracy was observed among [210].

^{99m}Tc-glucoheptonate (GHA) SPECT is a low-cost radiopharmaceutical agent that can be
strongly recommended for detecting residual tumors after surgery/radiotherapy and
progression [211].

^{99m}TcMDM (bis-methionine-DTPA) SPECT had a comparable sensitivity and specificity to
DSC (92% and 79% for MDM SPECT and 92% and 71% for DSC MRI) [212].

10

8. True progression vs pseudoprogression

11 Differentiating PsP from TP remains a persistent challenge in routine clinical practice. Some 12 radiological techniques with variable sensitivity, specificity and accuracy are available to help 13 clinicians (Table 6). According to this literature review, Figure 1 proposes a decision diagram 14 to orient clinical decision-making and assist with the distinction between PsP and TP. The 15 order of radiological imaging features proposed was based on the specificity and PPV of the different radiological examinations in the literature. Based on the RANO and modified 16 17 RANO criteria for the response assessment, conventional MRI results associated with clinical 18 evaluation and corticosteroid use were the three conventional and routinely used criteria to 19 differentiate PsP and TP [34,37]. In addition to those criteria, MGMT promoter methylation 20 status could help inform the diagnosis. Indeed, some authors identified MGMT promoter 21 methylation as a molecular marker and found that approximately two-thirds of MGMT-22 methylated tumors exhibited PsP [15,23,112,119,158,213-217], and an MRI suggesting 23 progression was associated with a 3.5-fold increased risk of having PsP rather than TP [216]. 24 In the case of inconclusive results, additional radiological parameters could help clinicians 25 diagnose TP versus PsP. Traditionally, the first step of those complementary exams consisted

1 of diffusion and perfusion MRI. According to the literature, the mean ADC value, ADC ratio 2 and mean rCBV suggested TP if they showed values of <1.28-1.33, <1.40-1.55 and >1.82-3 3.01, respectively (Tables 2 and 3, Figure 1). In case of remaining PsP doubt, MRS and PET 4 scans could provide supplementary information as a second step. The proposed MRS ratios to 5 differentiate PsP and TP were Cho/NAA and Cho/Cr, with Cho/NAA <1.47-2.11 and Cho/Cr 6 <0.82-2.25 indicating PsP according to the literature data (Table 4, Figure 1). PET scan 7 evaluation offers numerous metabolic tracers with higher diagnostic accuracy than FDG, such 8 as MET, FET or FDOPA. Finally, this review demonstrated that multiparametric imaging was 9 the best way to differentiate PsP from TP. However, some additional effort and research are 10 needed to increase the accuracy of the different modalities, and machine learning could 11 resolve this issue.

12 Radiomic features combined with clinical and genomic features could improve the diagnostic 13 differentiation between PsP and TP [218–220]. Some authors developed machine learning 14 models to improve PsP versus TP differentiation. Hu et al. analyzed multimodal MRI data 15 from 31 GBM patients (15 with TP and 16 with PsP) and developed a machine learning 16 algorithm to identify PsP versus TP with a sensitivity of 89.9% and a specificity of 93.7%, respectively [101]. Elshafeey et al. retrospectively demonstrated an accuracy of 90.8% for 17 18 perfusion MRI data coupled with a support vector machine as a radiomic model to distinguish 19 PsP and TP by analyzing data from 98 GBM patients [218]. Bacchi et al. conducted a pilot 20 study in 55 HGG patients combining MRI sequences and identified that deep learning models 21 based on DWI+FLAIR had higher accuracy (0.82), DWI+FLAIR and ADC had higher 22 sensitivity (1.00) and DWI+FLAIR had higher specificity (1.00) [221]. Gao et al. developed a 23 deep learning methodology using a deep neural network independent of handcrafting and 24 segmentation for the automated distinction between PsP and TP based on routine multimodal 25 MRI with a retrospective study of 146 GBM patients (66% TP and 34% after pathological

1 examination). The sensitivity, specificity and accuracy were 0.96, 0.80 and 0.90, respectively, 2 which were significantly higher than those associated with neurosurgeon interpretation [222]. 3 Bani-Sadr et al. showed that MGMT promoter status improved a machine learning model 4 based on conventional radiomics MRI [223]. Advances in neurooncology radiomics were 5 supported by available data from The Cancer Imaging Archive (TCIA) [224] and incorporated 6 tumor segmentation, tumor classification, treatment response assessment, prognostication and 7 therapeutic decisions [225]. The differentiation of PsP from TP was crucial, and machine 8 learning approaches incorporating multiple MRI data possibly associated with other imaging 9 modality data [226], clinical data and genomics [223] seemed to increase this challenging 10 task, even if additional studies with large patient samples were needed [62,225,227–230].

11 Currently, the only way to diagnose PsP versus TP with certainty is a histopathological 12 analysis. However, neurosurgery and neurobiopsy have associated morbidity and mortality, and the use of a noninvasive method to discern PsP and TP with fewer adverse effects seems 13 14 essential. Compared to surgery, gadolinium-based contrast agents used for MR imaging have 15 fewer and less common issues [231] such as the rare risk of nephrogenic systemic fibrosis 16 [232], deposition/retention of gadolinium in organs [233,234], environmental contamination 17 [235,236], post-contrast acute kidney injury, and allergic reaction [237]. However, 18 neurosurgery complications are numerous and more frequent, especially in the elderly, such 19 as postoperative hemorrhages (intraparenchymal, subdural and epidural), cerebrospinal fluid 20 leakage, pulmonary embolism, new postoperative neurological deficits, epilepsy, weakness, 21 and classical perioperative complications [238-245]. GBM exhibited high heterogeneity, 22 which could not be reflected in biopsy. Neurobiopsy could fail TP vs. PsP diagnosis, as they 23 are noninformative in 3% to 6% of cases with complications such as brain hemorrhage (5% to 24 9% cases), infection (<1% cases), and neurological deficit (2% to 6% cases), and neurobiopsy 25 is associated with a mortality rate from 0.4% to 2% [246–260].

1 Because biopsy, an invasive procedure, may not reflect the complete molecular features of the 2 evolving GBM tumor (60% to 70% of GBM mutations are not present across all regions of a 3 tumor [261]) and the distinction between PsP and TP is not always possible; therefore, 4 radiological imaging and blood-based biomarkers could be interesting, as they improve 5 specificity and decrease morbidity and mortality [262]. Some authors have shown that liquid 6 biopsies from blood, cerebrospinal fluid (CSF) or urinary fluid containing circulating 7 biomarkers are noninvasive or minimally invasive, quick and inexpensive methods that could 8 be more representative of the entire tumor and its heterogeneity [262,263] and useful for 9 GBM diagnosis and treatment monitoring [263–267].

10 Circulating biomarkers are represented by circulating tumor stem cells [268,269], circulating 11 cell-free nucleic acids [263] or circulating tumor cell clusters [270] with circulating tumor 12 cells (CTCs), circulating tumor DNA (ctDNA), cell-free DNA or extracellular vesicles (EVs) 13 [271–274]. These biomarkers could help to guide the diagnosis between PsP and TP using a 14 genomic analysis. Raza et al. analyzed 58 studies and 1853 patients and identified 133 15 biomarkers of GBM and 38 biomarkers for the differentiation of TP versus PsP [275]. CTCs 16 were described to contribute to tumorigenesis and recurrence in GBM [269,276]. Even if 17 CTCs are rare and challenging to isolate, with 20-82% sensitivity in blood [262], they can 18 provide information on protein, DNA or RNA levels, and guide therapeutic decisions 19 [277.278]. The isolation of CTCs [279] could be useful during follow-up [262,279–282] as a 20 complement to radiographic features [283]. However, the molecular information obtained 21 may not be representative of the entire GBM [265]. EVs (exosomes or microvesicles) are not 22 exclusively released from tumor cells. EVs contain nucleic acid biomarkers and protein 23 biomarkers and participate in angiogenesis, resistance to apoptosis, and proliferation 24 [262,267,278,284–289]. The authors showed that the EV detection sensitivity and specificity in blood and CSF were 28-91.7% and 86-100% and 61-87% and 93-100%, respectively [290]. 25

1 EVs have a very short half-life, which could reflect rapid changes in GBM biology [262]. The 2 authors also reported that IDH1 mutation, EGFR amplification or BRAF and KRAS mutation 3 could guide GBM diagnosis, glioma grading and assist in monitoring response assessment 4 [291]. EV analysis could be promising in the differentiation between PsP and TP [292]. The 5 authors demonstrated higher EV plasma levels in GBM patients, which decreased after 6 surgery and increased in the case of progression [293]. Koch et al. concluded that 7 microvesicle counts were significantly lower in PsP patients than in TP patients (p=0.014) in 8 a prospective study of 11 GBM patients [292]. Ct DNA is easier to detect, particularly in 9 CSF, but it has a short half-life [262,265]. The authors reported a sensitivity and specificity of 10 ctDNA detection in blood and CSF of 50-60% and 100% and 58-87% and 97-100%, 11 respectively [290]. CtDNA allows the identification of various mutations, such as IDH1 12 mutation, PTEN mutation, MGMT methylation or EGFR amplification [278,290,294]. The 13 levels of ctDNA were correlated with disease stage, and ctDNA allowed response assessment 14 evaluation [295]. Circulating miRNAs derived from CSF or blood [290] were studied as 15 biomarkers of GBM [262,272,296–300]; they were correlated with tumor grading [301,302], 16 tumor volume [303], treatment response [302,304] with restored levels after CRT [302], 17 conferred chemoresistance [304], prognosis [301] and survival [301]. Swellan et al. 18 concluded that miR-221 and miR-222 were increased in progressive disease versus stable 19 disease, complete response or partial response to treatment [305]. Circulating microRNA 20 analysis could be interesting for identifying TP versus PsP because miRNA accurately 21 identifies cancer tissue [175,262,275]. A prospective study of 91 gliomas showed that miRNA 22 levels did not increase in cases of PsP compared to TP [303]. A literature review showed that 23 circulating biomarkers could provide GBM management and facilitate initial and recurrence 24 diagnosis, tumor response assessment, genomic and molecular evolution tracking and PsP 25 identification [306]. Implementation in clinical practice could improve personalized medicine in terms of diagnosis, treatment, and follow-up. However, limitations of liquid biopsy persist
and the lack of reproducibility, consensus and standardization of biological fluid type (blood,
serum, CSF, urinary), nucleic acid type, and analytical technique (extraction methods,
measurement methods) remain [263,301,302]. Many studies were in vitro and not in vivo, and
cohort sizes were limited [265,287]. Additional studies seem necessary before clinical use.

9. Conclusion

6

7 PsP doubt is a common situation in clinical routines, and clinicians need uniform and 8 standardized criteria to confirm this diagnosis. The use of advanced radiological imaging and 9 imaging biomarkers is promising in this context and provides pathophysiological information. 10 This report demonstrated the superiority of advanced MRI techniques and PET for the 11 diagnosis of PsP, but efforts to create uniform practices and protocols are necessary. It is 12 essential that imaging is available, accessible, reproducible, and cost-effective. This review of 13 the literature indicates that there was no rigorous methodology to guide researchers and 14 provide comparable results based on the large number of parameter cutoff values, different 15 imaging protocols, small sample sizes, different population characteristics, and a lack of study 16 reproducibility. The variability in the extent of isotopes for TEP and SPECT and sequences 17 for MRI, multiplied by the large numbers of metrics evaluated, is significant. Algorithms 18 proposed by artificial intelligence and radiomics were used to analyze the results and improve 19 the usefulness of the data.

20 **Conflict of interest statement**

21 None

22 Funding source

This research did not receive any specific grant from funding agencies in the public,commercial, or not-for-profit sectors.

25 Abbreviations

- **ADC**: Apparent Diffusion Coefficient
- 2 ASL: Arterial Spin Labeling
- **BPTI**: International Brain Tumor Imaging
- **CBF**: Cerebral Blood Flow
- **CBV**: Cerebral Blood Volume
- **CE**: Contrast Enhancement
- **CEL**: contrast enhanced lesion
- **CRT**: Chemoradiotherapy
- **CT**: Computed Tomography
- **DCE**: Dynamic Contrast Enhanced
- **DSC**: Dynamic Susceptibility Contrast
- **DTI**: Diffusion Tensor Imaging
- **DWI**: Diffusion Weight Imaging
- **FA**: Fractional Anisotropy
- **FDG**: Fluoro-Deoxy-Glucose
- **FDOPA**: Fluoro-L-Dopa
- **FET**: Fluoroethyl-L-Tyrosine
- **FLT**: F-Fluorothymidine
- **FMISO**: F-fluoromisonidazole
- **GBM**: Glioblastoma
- 21 HGG: High Grade Glioma
- 22 Kep: Transfer constant from the extracellular-extravascular space into the plasma
- 23 K^{trans}: Volume Transfer Constant
- **MET**: methyl-L-methionine
- 25 MRI: Magnetic Resonance Imaging

- 1 MRS: Magnetic Resonance Spectroscopy
- **PET**: Positron Emission Tomography
- **PsP**: Pseusoprogression
- **RT**: Radiotherapy
- **SPECT**: Single Photon Emission Computed Tomography
- **SUV**: Standardized Uptake Value
- **SWI**: Susceptibility-weighted imaging
- **TBR**: Tumor to Brain Ratio
- **TMZ**: Temozolomide
- **TNR**: Tumor-to-Normal brain Ratio
- **TP**: True Progression
- 12 Ve: Volume of extravascular-extracellular space
- 13 V_p: Vascular plasma volume

References

1. Siegel RL, Miller KD, Jemal A. Cancer statistics, 2020. CA Cancer J Clin. 2020;70(1):7–30.

2. Ostrom QT, Gittleman H, Stetson L, Virk SM, Barnholtz-Sloan JS. Epidemiology of gliomas. Cancer Treat Res. 2015;163:1–14.

3. Ostrom QT, Gittleman H, Farah P, Ondracek A, Chen Y, Wolinsky Y, et al. CBTRUS statistical report: Primary brain and central nervous system tumors diagnosed in the United States in 2006-2010. Neuro-Oncol. 2013 Nov;15 Suppl 2:ii1-56.

4. Ahmed R, Oborski MJ, Hwang M, Lieberman FS, Mountz JM. Malignant gliomas: current perspectives in diagnosis, treatment, and early response assessment using advanced quantitative imaging methods. Cancer Manag Res. 2014;6:149–70.

5. Dolecek TA, Propp JM, Stroup NE, Kruchko C. CBTRUS Statistical Report: Primary Brain and Central Nervous System Tumors Diagnosed in the United States in 2005–2009. Neuro-Oncol. 2012 Nov 1;14(suppl_5):v1–49.

6. Albert NL, Weller M, Suchorska B, Galldiks N, Soffietti R, Kim MM, et al. Response Assessment in Neuro-Oncology working group and European Association for Neuro-Oncology recommendations for the clinical use of PET imaging in gliomas. Neuro-Oncol. 2016;18(9):1199–208.

7. Bleeker FE, Molenaar RJ, Leenstra S. Recent advances in the molecular understanding of glioblastoma. J Neurooncol. 2012 May;108(1):11–27.

8. Stupp R, Mason WP, van den Bent MJ, Weller M, Fisher B, Taphoorn MJB, et al. Radiotherapy plus concomitant and adjuvant temozolomide for glioblastoma. N Engl J Med. 2005 Mar 10;352(10):987–96.

9. Seystahl K, Wick W, Weller M. Therapeutic options in recurrent glioblastoma--An update. Crit Rev Oncol Hematol. 2016 Mar;99:389–408.

10. Tamimi AF, Juweid M. Epidemiology and Outcome of Glioblastoma. In: De Vleeschouwer S, editor. Glioblastoma [Internet]. Brisbane (AU): Codon Publications; 2017 [cited 2020 Nov 21]. Available from: http://www.ncbi.nlm.nih.gov/books/NBK470003/

11. Hanif F, Muzaffar K, Perveen K, Malhi SM, Simjee SU. Glioblastoma Multiforme: A Review of its Epidemiology and Pathogenesis through Clinical Presentation and Treatment. Asian Pac J Cancer Prev APJCP. 2017 01;18(1):3–9.

12. Witthayanuwat S, Pesee M, Supaadirek C, Supakalin N, Thamronganantasakul K, Krusun S. Survival Analysis of Glioblastoma Multiforme. Asian Pac J Cancer Prev APJCP. 2018 Sep 26;19(9):2613–7.

13. Stupp R, Hegi ME, Mason WP, van den Bent MJ, Taphoorn MJB, Janzer RC, et al. Effects of radiotherapy with concomitant and adjuvant temozolomide versus radiotherapy alone on survival in glioblastoma in a randomised phase III study: 5-year analysis of the EORTC-NCIC trial. Lancet Oncol. 2009 May;10(5):459–66.

14. Tykocki T, Eltayeb M. Ten-year survival in glioblastoma. A systematic review. J Clin Neurosci Off J Neurosurg Soc Australas. 2018 Aug;54:7–13.

15. Brandes AA, Franceschi E, Tosoni A, Blatt V, Pession A, Tallini G, et al. MGMT promoter methylation status can predict the incidence and outcome of pseudoprogression after concomitant radiochemotherapy in newly diagnosed glioblastoma patients. J Clin Oncol Off J Am Soc Clin Oncol. 2008 May 1;26(13):2192–7.

16. Chamberlain MC, Glantz MJ, Chalmers L, Van Horn A, Sloan AE. Early necrosis following concurrent Temodar and radiotherapy in patients with glioblastoma. J Neurooncol. 2007 Mar;82(1):81–3.

17. Taal W, Brandsma D, de Bruin HG, Bromberg JE, Swaak-Kragten AT, Smitt PAES, et al. Incidence of early pseudo-progression in a cohort of malignant glioma patients treated

with chemoirradiation with temozolomide. Cancer. 2008 Jul 15;113(2):405-10.

18. Wick W, Chinot OL, Bendszus M, Mason W, Henriksson R, Saran F, et al. Evaluation of pseudoprogression rates and tumor progression patterns in a phase III trial of bevacizumab plus radiotherapy/temozolomide for newly diagnosed glioblastoma. Neuro-Oncol. 2016;18(10):1434–41.

19. Brandsma D, Stalpers L, Taal W, Sminia P, van den Bent MJ. Clinical features, mechanisms, and management of pseudoprogression in malignant gliomas. Lancet Oncol. 2008 May;9(5):453–61.

20. Rowe LS, Butman JA, Mackey M, Shih JH, Cooley-Zgela T, Ning H, et al. Differentiating pseudoprogression from true progression: analysis of radiographic, biologic, and clinical clues in GBM. J Neurooncol. 2018 May 16;

21. Chaskis C, Neyns B, Michotte A, De Ridder M, Everaert H. Pseudoprogression after radiotherapy with concurrent temozolomide for high-grade glioma: clinical observations and working recommendations. Surg Neurol. 2009 Oct;72(4):423–8.

22. Chang JH, Kim C-Y, Choi BS, Kim YJ, Kim JS, Kim IA. Pseudoprogression and pseudoresponse in the management of high-grade glioma : optimal decision timing according to the response assessment of the neuro-oncology working group. J Korean Neurosurg Soc. 2014 Jan;55(1):5–11.

23. Zikou A, Sioka C, Alexiou GA, Fotopoulos A, Voulgaris S, Argyropoulou MI. Radiation Necrosis, Pseudoprogression, Pseudoresponse, and Tumor Recurrence: Imaging Challenges for the Evaluation of Treated Gliomas. Contrast Media Mol Imaging. 2018;2018:6828396.

24. Nasseri M, Gahramanov S, Netto JP, Fu R, Muldoon LL, Varallyay C, et al. Evaluation of pseudoprogression in patients with glioblastoma multiforme using dynamic magnetic resonance imaging with ferumoxytol calls RANO criteria into question. Neuro-Oncol. 2014 Aug;16(8):1146–54.

25. Jefferies S, Burton K, Jones P, Burnet N. Interpretation of Early Imaging after Concurrent Radiotherapy and Temozolomide for Glioblastoma. Clin Oncol. 2007 Apr 1;19(3):S33.

26. Radbruch A, Fladt J, Kickingereder P, Wiestler B, Nowosielski M, Bäumer P, et al. Pseudoprogression in patients with glioblastoma: clinical relevance despite low incidence. Neuro-Oncol. 2015 Jan;17(1):151–9.

27. Tran DKT, Jensen RL. Treatment-related brain tumor imaging changes: So-called "pseudoprogression" vs. tumor progression: Review and future research opportunities. Surg Neurol Int. 2013;4(Suppl 3):S129-135.

28. Larsen VA, Simonsen HJ, Law I, Larsson HBW, Hansen AE. Evaluation of dynamic contrast-enhanced T1-weighted perfusion MRI in the differentiation of tumor recurrence from radiation necrosis. Neuroradiology. 2013 Feb;55(3):361–9.

29. Hygino da Cruz LC, Rodriguez I, Domingues RC, Gasparetto EL, Sorensen AG. Pseudoprogression and pseudoresponse: imaging challenges in the assessment of posttreatment glioma. AJNR Am J Neuroradiol. 2011 Dec;32(11):1978–85.

30. Jahangiri A, Aghi MK. Pseudoprogression and treatment effect. Neurosurg Clin N Am. 2012 Apr;23(2):277–87, viii–ix.

31. Abbasi AW, Westerlaan HE, Holtman GA, Aden KM, van Laar PJ, van der Hoorn A. Incidence of Tumour Progression and Pseudoprogression in High-Grade Gliomas:

a Systematic Review and Meta-Analysis. Clin Neuroradiol. 2018 Sep;28(3):401–11.

32. Thust SC, van den Bent MJ, Smits M. Pseudoprogression of brain tumors. J Magn Reson Imaging JMRI. 2018 May 7;

33. Wen PY, Chang SM, Van den Bent MJ, Vogelbaum MA, Macdonald DR, Lee EQ. Response Assessment in Neuro-Oncology Clinical Trials. J Clin Oncol Off J Am Soc Clin

Oncol. 2017 Jul 20;35(21):2439–49.

34. Wen PY, Macdonald DR, Reardon DA, Cloughesy TF, Sorensen AG, Galanis E, et al. Updated response assessment criteria for high-grade gliomas: response assessment in neurooncology working group. J Clin Oncol Off J Am Soc Clin Oncol. 2010 Apr 10;28(11):1963– 72.

35. Macdonald DR, Cascino TL, Schold SC, Cairneross JG. Response criteria for phase II studies of supratentorial malignant glioma. J Clin Oncol Off J Am Soc Clin Oncol. 1990 Jul;8(7):1277–80.

36. Ellingson BM, Bendszus M, Boxerman J, Barboriak D, Erickson BJ, Smits M, et al. Consensus recommendations for a standardized Brain Tumor Imaging Protocol in clinical trials. Neuro-Oncol. 2015 Sep;17(9):1188–98.

37. Ellingson BM, Wen PY, Cloughesy TF. Modified Criteria for Radiographic Response Assessment in Glioblastoma Clinical Trials. Neurother J Am Soc Exp Neurother. 2017;14(2):307–20.

38. Lieberman F. Glioblastoma update: molecular biology, diagnosis, treatment, response assessment, and translational clinical trials. F1000Research [Internet]. 2017 Oct 26 [cited 2018 Sep 3];6. Available from: https://www.ncbi.nlm.nih.gov/pmc/articles/PMC5658706/

39. Masch WR, Wang PI, Chenevert TL, Junck L, Tsien C, Heth JA, et al. Comparison of Diffusion Tensor Imaging and Magnetic Resonance Perfusion Imaging in Differentiating Recurrent Brain Neoplasm From Radiation Necrosis. Acad Radiol. 2016 May;23(5):569–76.

40. Shukla G, Alexander GS, Bakas S, Nikam R, Talekar K, Palmer JD, et al. Advanced magnetic resonance imaging in glioblastoma: a review. Chin Clin Oncol. 2017 Aug;6(4):40.
41. Hyare H, Thust S, Rees J. Advanced MRI Techniques in the Monitoring of Treatment

of Gliomas. Curr Treat Options Neurol. 2017 Mar;19(3):11.

42. van Dijken BRJ, van Laar PJ, Holtman GA, van der Hoorn A. Diagnostic accuracy of magnetic resonance imaging techniques for treatment response evaluation in patients with high-grade glioma, a systematic review and meta-analysis. Eur Radiol. 2017 Oct;27(10):4129–44.

43. Neal ML, Trister AD, Ahn S, Baldock A, Bridge CA, Guyman L, et al. Response classification based on a minimal model of glioblastoma growth is prognostic for clinical outcomes and distinguishes progression from pseudoprogression. Cancer Res. 2013 May 15;73(10):2976–86.

44. Ellingson BM, Chung C, Pope WB, Boxerman JL, Kaufmann TJ. Pseudoprogression, radionecrosis, inflammation or true tumor progression? challenges associated with glioblastoma response assessment in an evolving therapeutic landscape. J Neurooncol. 2017 Sep;134(3):495–504.

45. Santra A, Kumar R, Sharma P, Bal C, Kumar A, Julka PK, et al. F-18 FDG PET-CT in patients with recurrent glioma: comparison with contrast enhanced MRI. Eur J Radiol. 2012 Mar;81(3):508–13.

46. https://www.nccn.org/professionals/physi- cian_gls/f_guidelines.asp#cns.

47. Agarwal A, Kumar S, Narang J, Schultz L, Mikkelsen T, Wang S, et al. Morphologic MRI features, diffusion tensor imaging and radiation dosimetric analysis to differentiate pseudo-progression from early tumor progression. J Neurooncol. 2013 May;112(3):413–20.
48. Gladwish A, Koh E-S, Hoisak J, Lockwood G, Millar B-A, Mason W, et al.

Evaluation of early imaging response criteria in glioblastoma multiforme. Radiat Oncol Lond Engl. 2011 Sep 23;6:121.

49. Mullins ME, Barest GD, Schaefer PW, Hochberg FH, Gonzalez RG, Lev MH. Radiation necrosis versus glioma recurrence: conventional MR imaging clues to diagnosis. AJNR Am J Neuroradiol. 2005 Sep;26(8):1967–72.

50. Young RJ, Gupta A, Shah AD, Graber JJ, Zhang Z, Shi W, et al. Potential utility of

conventional MRI signs in diagnosing pseudoprogression in glioblastoma. Neurology. 2011 May 31;76(22):1918–24.

51. Kim HS, Goh MJ, Kim N, Choi CG, Kim SJ, Kim JH. Which combination of MR imaging modalities is best for predicting recurrent glioblastoma? Study of diagnostic accuracy and reproducibility. Radiology. 2014 Dec;273(3):831–43.

52. Reddy K, Westerly D, Chen C. MRI patterns of T1 enhancing radiation necrosis versus tumour recurrence in high-grade gliomas. J Med Imaging Radiat Oncol. 2013 Jun;57(3):349–55.

53. Hansen MR, Pan E, Wilson A, McCreary M, Wang Y, Stanley T, et al. Postgadolinium 3-dimensional spatial, surface, and structural characteristics of glioblastomas differentiate pseudoprogression from true tumor progression. J Neurooncol. 2018 Jun 7;

54. Chen X, Wei X, Zhang Z, Yang R, Zhu Y, Jiang X. Differentiation of true-progression from pseudoprogression in glioblastoma treated with radiation therapy and concomitant temozolomide by GLCM texture analysis of conventional MRI. Clin Imaging. 2015 Oct;39(5):775–80.

55. Zaki HS, Jenkinson MD, Du Plessis DG, Smith T, Rainov NG. Vanishing contrast enhancement in malignant glioma after corticosteroid treatment. Acta Neurochir (Wien). 2004 Aug;146(8):841–5.

56. de Groot JF, Fuller G, Kumar AJ, Piao Y, Eterovic K, Ji Y, et al. Tumor invasion after treatment of glioblastoma with bevacizumab: radiographic and pathologic correlation in humans and mice. Neuro-Oncol. 2010 Mar;12(3):233–42.

57. Ito-Yamashita T, Nakasu Y, Mitsuya K, Mizokami Y, Namba H. Detection of tumor progression by signal intensity increase on fluid-attenuated inversion recovery magnetic resonance images in the resection cavity of high-grade gliomas. Neurol Med Chir (Tokyo). 2013;53(7):496–500.

58. Abel R, Jones J, Mandelin P, Cen S, Pagnini P. Distinguishing Pseudoprogression From True Progression by FLAIR Volumetric Characteristics Compared to 45 Gy Isodose Volumes in Treated Glioblastoma Patients. Int J Radiat Oncol • Biol • Phys. 2012 Nov 1;84(3):S275.

59. Abdulla S, Saada J, Johnson G, Jefferies S, Ajithkumar T. Tumour progression or pseudoprogression? A review of post-treatment radiological appearances of glioblastoma. Clin Radiol. 2015 Nov;70(11):1299–312.

60. Oberheim Bush NA, Cha S, Chang SM, Clarke JL. Chapter 55 - Pseudoprogression in Neuro-Oncology: Overview, Pathophysiology, and Interpretation. In: Newton HB, editor. Handbook of Neuro-Oncology Neuroimaging (Second Edition) [Internet]. San Diego: Academic Press; 2016 [cited 2019 Jun 13]. p. 681–95. Available from:

http://www.sciencedirect.com/science/article/pii/B9780128009451000550

61. Gerstner ER, McNamara MB, Norden AD, Lafrankie D, Wen PY. Effect of adding temozolomide to radiation therapy on the incidence of pseudo-progression. J Neurooncol. 2009 Aug;94(1):97–101.

62. Zhang J, Yu H, Qian X, Liu K, Tan H, Yang T, et al. Pseudo progression identification of glioblastoma with dictionary learning. Comput Biol Med. 2016 01;73:94–101.

63. Verma R, Zacharaki EI, Ou Y, Cai H, Chawla S, Lee S-K, et al. Multiparametric tissue characterization of brain neoplasms and their recurrence using pattern classification of MR images. Acad Radiol. 2008 Aug;15(8):966–77.

64. Asao C, Korogi Y, Kitajima M, Hirai T, Baba Y, Makino K, et al. Diffusion-weighted imaging of radiation-induced brain injury for differentiation from tumor recurrence. AJNR Am J Neuroradiol. 2005 Jul;26(6):1455–60.

65. Lee WJ, Choi SH, Park C-K, Yi KS, Kim TM, Lee S-H, et al. Diffusion-weighted MR imaging for the differentiation of true progression from pseudoprogression following

concomitant radiotherapy with temozolomide in patients with newly diagnosed high-grade gliomas. Acad Radiol. 2012 Nov;19(11):1353–61.

66. Xu J-L, Li Y-L, Lian J-M, Dou S, Yan F-S, Wu H, et al. Distinction between postoperative recurrent glioma and radiation injury using MR diffusion tensor imaging. Neuroradiology. 2010 Dec;52(12):1193–9.

67. Hein PA, Eskey CJ, Dunn JF, Hug EB. Diffusion-weighted imaging in the follow-up of treated high-grade gliomas: tumor recurrence versus radiation injury. AJNR Am J Neuroradiol. 2004 Feb;25(2):201–9.

68. Sundgren PC, Fan X, Weybright P, Welsh RC, Carlos RC, Petrou M, et al. Differentiation of recurrent brain tumor versus radiation injury using diffusion tensor imaging in patients with new contrast-enhancing lesions. Magn Reson Imaging. 2006 Nov;24(9):1131–42.

69. Chenevert TL, Stegman LD, Taylor JM, Robertson PL, Greenberg HS, Rehemtulla A, et al. Diffusion magnetic resonance imaging: an early surrogate marker of therapeutic efficacy in brain tumors. J Natl Cancer Inst. 2000 Dec 20;92(24):2029–36.

70. Huang RY, Neagu MR, Reardon DA, Wen PY. Pitfalls in the neuroimaging of glioblastoma in the era of antiangiogenic and immuno/targeted therapy - detecting illusive disease, defining response. Front Neurol. 2015;6:33.

71. Yamasaki F, Kurisu K, Satoh K, Arita K, Sugiyama K, Ohtaki M, et al. Apparent diffusion coefficient of human brain tumors at MR imaging. Radiology. 2005 Jun;235(3):985–91.

72. Sugahara T, Korogi Y, Kochi M, Ikushima I, Shigematu Y, Hirai T, et al. Usefulness of diffusion-weighted MRI with echo-planar technique in the evaluation of cellularity in gliomas. J Magn Reson Imaging JMRI. 1999 Jan;9(1):53–60.

73. Reimer C, Deike K, Graf M, Reimer P, Wiestler B, Floca RO, et al. Differentiation of pseudoprogression and real progression in glioblastoma using ADC parametric response maps. PLoS ONE [Internet]. 2017 Apr 6 [cited 2019 Apr 28];12(4). Available from: https://www.ncbi.nlm.nih.gov/pmc/articles/PMC5383222/

74. Zeng Q-S, Li C-F, Liu H, Zhen J-H, Feng D-C. Distinction between recurrent glioma and radiation injury using magnetic resonance spectroscopy in combination with diffusion-weighted imaging. Int J Radiat Oncol Biol Phys. 2007 May 1;68(1):151–8.

75. Jena A, Taneja S, Jha A, Damesha NK, Negi P, Jadhav GK, et al. Multiparametric Evaluation in Differentiating Glioma Recurrence from Treatment-Induced Necrosis Using Simultaneous 18F-FDG-PET/MRI: A Single-Institution Retrospective Study. AJNR Am J Neuroradiol. 2017 May;38(5):899–907.

76. Fink JR, Carr RB, Matsusue E, Iyer RS, Rockhill JK, Haynor DR, et al. Comparison of 3 Tesla proton MR spectroscopy, MR perfusion and MR diffusion for distinguishing glioma recurrence from posttreatment effects. J Magn Reson Imaging JMRI. 2012 Jan;35(1):56–63.

77. Prager AJ, Martinez N, Beal K, Omuro A, Zhang Z, Young RJ. Diffusion and perfusion MRI to differentiate treatment-related changes including pseudoprogression from recurrent tumors in high-grade gliomas with histopathologic evidence. AJNR Am J Neuroradiol. 2015 May;36(5):877–85.

78. Alexiou GA, Zikou A, Tsiouris S, Goussia A, Kosta P, Papadopoulos A, et al. Comparison of diffusion tensor, dynamic susceptibility contrast MRI and (99m)Tc-Tetrofosmin brain SPECT for the detection of recurrent high-grade glioma. Magn Reson Imaging. 2014 Sep;32(7):854–9.

79. Bulik M, Kazda T, Slampa P, Jancalek R. The Diagnostic Ability of Follow-Up Imaging Biomarkers after Treatment of Glioblastoma in the Temozolomide Era: Implications from Proton MR Spectroscopy and Apparent Diffusion Coefficient Mapping [Internet].

BioMed Research International. 2015 [cited 2019 Apr 28]. Available from: https://www.hindawi.com/journals/bmri/2015/641023/

80. Kazda T, Bulik M, Pospisil P, Lakomy R, Smrcka M, Slampa P, et al. Advanced MRI increases the diagnostic accuracy of recurrent glioblastoma: Single institution thresholds and validation of MR spectroscopy and diffusion weighted MR imaging. NeuroImage Clin. 2016;11:316–21.

81. Bobek-Billewicz B, Stasik-Pres G, Majchrzak H, Zarudzki L. Differentiation between brain tumor recurrence and radiation injury using perfusion, diffusion-weighted imaging and MR spectroscopy. Folia Neuropathol. 2010;48(2):81–92.

82. Al Sayyari A, Buckley R, McHenery C, Pannek K, Coulthard A, Rose S. Distinguishing recurrent primary brain tumor from radiation injury: a preliminary study using a susceptibility-weighted MR imaging-guided apparent diffusion coefficient analysis strategy. AJNR Am J Neuroradiol. 2010 Jun;31(6):1049–54.

83. Song YS, Choi SH, Park C-K, Yi KS, Lee WJ, Yun TJ, et al. True progression versus pseudoprogression in the treatment of glioblastomas: a comparison study of normalized cerebral blood volume and apparent diffusion coefficient by histogram analysis. Korean J Radiol. 2013 Aug;14(4):662–72.

84. Chu HH, Choi SH, Ryoo I, Kim SC, Yeom JA, Shin H, et al. Differentiation of true progression from pseudoprogression in glioblastoma treated with radiation therapy and concomitant temozolomide: comparison study of standard and high-b-value diffusion-weighted imaging. Radiology. 2013 Dec;269(3):831–40.

85. Wang S, Martinez-Lage M, Sakai Y, Chawla S, Kim SG, Alonso-Basanta M, et al. Differentiating Tumor Progression from Pseudoprogression in Patients with Glioblastomas Using Diffusion Tensor Imaging and Dynamic Susceptibility Contrast MRI. AJNR Am J Neuroradiol. 2016 Jan;37(1):28–36.

86. Thust SC, Heiland S, Falini A, Jäger HR, Waldman AD, Sundgren PC, et al. Glioma imaging in Europe: A survey of 220 centres and recommendations for best clinical practice. Eur Radiol. 2018 Aug;28(8):3306–17.

87. Fatterpekar GM, Galheigo D, Narayana A, Johnson G, Knopp E. Treatment-related change versus tumor recurrence in high-grade gliomas: a diagnostic conundrum--use of dynamic susceptibility contrast-enhanced (DSC) perfusion MRI. AJR Am J Roentgenol. 2012 Jan;198(1):19–26.

88. Cha J, Kim ST, Kim H-J, Kim B-J, Kim YK, Lee JY, et al. Differentiation of tumor progression from pseudoprogression in patients with posttreatment glioblastoma using multiparametric histogram analysis. AJNR Am J Neuroradiol. 2014 Jul;35(7):1309–17.

89. Cha S, Knopp EA, Johnson G, Wetzel SG, Litt AW, Zagzag D. Intracranial mass lesions: dynamic contrast-enhanced susceptibility-weighted echo-planar perfusion MR imaging. Radiology. 2002 Apr;223(1):11–29.

90. Patel P, Baradaran H, Delgado D, Askin G, Christos P, John Tsiouris A, et al. MR perfusion-weighted imaging in the evaluation of high-grade gliomas after treatment: a systematic review and meta-analysis. Neuro-Oncol. 2017;19(1):118–27.

91. Barajas RF, Chang JS, Segal MR, Parsa AT, McDermott MW, Berger MS, et al. Differentiation of recurrent glioblastoma multiforme from radiation necrosis after external beam radiation therapy with dynamic susceptibility-weighted contrast-enhanced perfusion MR imaging. Radiology. 2009 Nov;253(2):486–96.

92. Seeger A, Braun C, Skardelly M, Paulsen F, Schittenhelm J, Ernemann U, et al. Comparison of three different MR perfusion techniques and MR spectroscopy for multiparametric assessment in distinguishing recurrent high-grade gliomas from stable disease. Acad Radiol. 2013 Dec;20(12):1557–65.

93. D'Souza MM, Sharma R, Jaimini A, Panwar P, Saw S, Kaur P, et al. 11C-MET

PET/CT and advanced MRI in the evaluation of tumor recurrence in high-grade gliomas. Clin Nucl Med. 2014 Sep;39(9):791–8.

94. Heidemans-Hazelaar C, Verbeek AY, Oosterkamp HM, Van der Kallen B, Vecht CJ. Use of perfusion MR imaging for differentiation between tumor progression and pseudoprogression in recurrent glioblastoma multiforme. J Clin Oncol. 2010 May 20;28(15_suppl):2026–2026.

95. Hu LS, Baxter LC, Smith KA, Feuerstein BG, Karis JP, Eschbacher JM, et al. Relative cerebral blood volume values to differentiate high-grade glioma recurrence from posttreatment radiation effect: direct correlation between image-guided tissue histopathology and localized dynamic susceptibility-weighted contrast-enhanced perfusion MR imaging measurements. AJNR Am J Neuroradiol. 2009 Mar;30(3):552–8.

96. Hu LS, Eschbacher JM, Heiserman JE, Dueck AC, Shapiro WR, Liu S, et al. Reevaluating the imaging definition of tumor progression: perfusion MRI quantifies recurrent glioblastoma tumor fraction, pseudoprogression, and radiation necrosis to predict survival. Neuro-Oncol. 2012 Jul;14(7):919–30.

97. Gasparetto EL, Pawlak MA, Patel SH, Huse J, Woo JH, Krejza J, et al. Posttreatment recurrence of malignant brain neoplasm: accuracy of relative cerebral blood volume fraction in discriminating low from high malignant histologic volume fraction. Radiology. 2009 Mar;250(3):887–96.

98. Gahramanov S, Raslan AM, Muldoon LL, Hamilton BE, Rooney WD, Varallyay CG, et al. Potential for differentiation of pseudoprogression from true tumor progression with dynamic susceptibility-weighted contrast-enhanced magnetic resonance imaging using ferumoxytol vs. gadoteridol: a pilot study. Int J Radiat Oncol Biol Phys. 2011 Feb 1;79(2):514–23.

99. Kim YH, Oh SW, Lim YJ, Park C-K, Lee S-H, Kang KW, et al. Differentiating radiation necrosis from tumor recurrence in high-grade gliomas: assessing the efficacy of 18F-FDG PET, 11C-methionine PET and perfusion MRI. Clin Neurol Neurosurg. 2010 Nov;112(9):758–65.

100. Young RJ, Gupta A, Shah AD, Graber JJ, Chan TA, Zhang Z, et al. MRI perfusion in determining pseudoprogression in patients with glioblastoma. Clin Imaging. 2013 Feb;37(1):41–9.

101. Hu X, Wong KK, Young GS, Guo L, Wong ST. Support vector machine multiparametric MRI identification of pseudoprogression from tumor recurrence in patients with resected glioblastoma. J Magn Reson Imaging JMRI. 2011 Feb;33(2):296–305.

102. Jain R, Scarpace L, Ellika S, Schultz LR, Rock JP, Rosenblum ML, et al. First-pass perfusion computed tomography: initial experience in differentiating recurrent brain tumors from radiation effects and radiation necrosis. Neurosurgery. 2007 Oct;61(4):778–86; discussion 786-787.

103. Boxerman JL, Ellingson BM, Jeyapalan S, Elinzano H, Harris RJ, Rogg JM, et al. Longitudinal DSC-MRI for Distinguishing Tumor Recurrence From Pseudoprogression in Patients With a High-grade Glioma. Am J Clin Oncol. 2017 Jun;40(3):228–34.

104. Tsien C, Galbán CJ, Chenevert TL, Johnson TD, Hamstra DA, Sundgren PC, et al. Parametric response map as an imaging biomarker to distinguish progression from pseudoprogression in high-grade glioma. J Clin Oncol Off J Am Soc Clin Oncol. 2010 May 1;28(13):2293–9.

105. Shin KE, Ahn KJ, Choi HS, Jung SL, Kim BS, Jeon SS, et al. DCE and DSC MR perfusion imaging in the differentiation of recurrent tumour from treatment-related changes in patients with glioma. Clin Radiol. 2014 Jun;69(6):e264-272.

106. Mangla R, Singh G, Ziegelitz D, Milano MT, Korones DN, Zhong J, et al. Changes in relative cerebral blood volume 1 month after radiation-temozolomide therapy can help predict

overall survival in patients with glioblastoma. Radiology. 2010 Aug;256(2):575-84.

107. Kong D-S, Kim ST, Kim E-H, Lim DH, Kim WS, Suh Y-L, et al. Diagnostic dilemma of pseudoprogression in the treatment of newly diagnosed glioblastomas: the role of assessing relative cerebral blood flow volume and oxygen-6-methylguanine-DNA methyltransferase promoter methylation status. AJNR Am J Neuroradiol. 2011 Feb;32(2):382–7.

108. Baek HJ, Kim HS, Kim N, Choi YJ, Kim YJ. Percent Change of Perfusion Skewness and Kurtosis: A Potential Imaging Biomarker for Early Treatment Response in Patients with Newly Diagnosed Glioblastomas. Radiology. 2012 Sep 1;264(3):834–43.

109. Suh CH, Kim HS, Choi YJ, Kim N, Kim SJ. Prediction of pseudoprogression in patients with glioblastomas using the initial and final area under the curves ratio derived from dynamic contrast-enhanced T1-weighted perfusion MR imaging. AJNR Am J Neuroradiol. 2013 Dec;34(12):2278–86.

110. Bisdas S, Naegele T, Ritz R, Dimostheni A, Pfannenberg C, Reimold M, et al. Distinguishing recurrent high-grade gliomas from radiation injury: a pilot study using dynamic contrast-enhanced MR imaging. Acad Radiol. 2011 May;18(5):575–83.

111. Yun TJ, Park C-K, Kim TM, Lee S-H, Kim J-H, Sohn C-H, et al. Glioblastoma treated with concurrent radiation therapy and temozolomide chemotherapy: differentiation of true progression from pseudoprogression with quantitative dynamic contrast-enhanced MR imaging. Radiology. 2015 Mar;274(3):830–40.

112. Thomas AA, Arevalo-Perez J, Kaley T, Lyo J, Peck KK, Shi W, et al. Dynamic contrast enhanced T1 MRI perfusion differentiates pseudoprogression from recurrent glioblastoma. J Neurooncol. 2015 Oct;125(1):183–90.

113. Choi YJ, Kim HS, Jahng G-H, Kim SJ, Suh DC. Pseudoprogression in patients with glioblastoma: added value of arterial spin labeling to dynamic susceptibility contrast perfusion MR imaging. Acta Radiol Stockh Swed 1987. 2013 May;54(4):448–54.

114. Yoo R-E, Choi SH. Recent Application of Advanced MR Imaging to Predict Pseudoprogression in High-grade Glioma Patients. Magn Reson Med Sci MRMS Off J Jpn Soc Magn Reson Med. 2016;15(2):165–77.

115. Jovanovic M, Radenkovic S, Stosic-Opincal T, Lavrnic S, Gavrilovic S, Lazovic-Popovic B, et al. Differentiation between progression and pseudoprogression by arterial spin labeling MRI in patients with glioblastoma multiforme. J BUON Off J Balk Union Oncol. 2017 Aug;22(4):1061–7.

116. Ozsunar Y, Mullins ME, Kwong K, Hochberg FH, Ament C, Schaefer PW, et al. Glioma recurrence versus radiation necrosis? A pilot comparison of arterial spin-labeled, dynamic susceptibility contrast enhanced MRI, and FDG-PET imaging. Acad Radiol. 2010 Mar;17(3):282–90.

117. Lewis R, Bhandari A, McKintosh E, Plowman P, Lansley J, Evanson J, et al. Differentiating tumour progression from pseudoprogression in patients with glioblastoma using multiparametric MRI imaging: Data from Barts Health NHS trust London. Eur J Surg Oncol. 2016 Nov 1;42(11):S248–9.

118. Park JE, Kim HS, Goh MJ, Kim SJ, Kim JH. Pseudoprogression in Patients with Glioblastoma: Assessment by Using Volume-weighted Voxel-based Multiparametric Clustering of MR Imaging Data in an Independent Test Set. Radiology. 2015 Jun;275(3):792–802.

119. Yoon RG, Kim HS, Paik W, Shim WH, Kim SJ, Kim JH. Different diagnostic values of imaging parameters to predict pseudoprogression in glioblastoma subgroups stratified by MGMT promoter methylation. Eur Radiol. 2017 Jan;27(1):255–66.

120. Varallyay CG, Muldoon LL, Gahramanov S, Wu YJ, Goodman JA, Li X, et al. Dynamic MRI using iron oxide nanoparticles to assess early vascular effects of antiangiogenic versus corticosteroid treatment in a glioma model. J Cereb Blood Flow Metab

Off J Int Soc Cereb Blood Flow Metab. 2009 Apr;29(4):853–60.

121. Gahramanov S, Muldoon LL, Varallyay CG, Li X, Kraemer DF, Fu R, et al. Pseudoprogression of glioblastoma after chemo- and radiation therapy: diagnosis by using dynamic susceptibility-weighted contrast-enhanced perfusion MR imaging with ferumoxytol versus gadoteridol and correlation with survival. Radiology. 2013 Mar;266(3):842–52.

122. Barajas RF, Hamilton BE, Schwartz D, McConnell HL, Pettersson DR, Horvath A, et al. Combined iron oxide nanoparticle ferumoxytol and gadolinium contrast enhanced MRI define glioblastoma pseudoprogression. Neuro-Oncol. 2019 Mar 18;21(4):517–26.

123. Ma B, Blakeley JO, Hong X, Zhang H, Jiang S, Blair L, et al. Applying amide proton transfer-weighted MRI to distinguish pseudoprogression from true progression in malignant gliomas. J Magn Reson Imaging JMRI. 2016;44(2):456–62.

124. Zhang H, Ma L, Wang Q, Zheng X, Wu C, Xu B-N. Role of magnetic resonance spectroscopy for the differentiation of recurrent glioma from radiation necrosis: a systematic review and meta-analysis. Eur J Radiol. 2014 Dec;83(12):2181–9.

125. Kamada K, Houkin K, Abe H, Sawamura Y, Kashiwaba T. Differentiation of cerebral radiation necrosis from tumor recurrence by proton magnetic resonance spectroscopy. Neurol Med Chir (Tokyo). 1997 Mar;37(3):250–6.

126. Rabinov JD, Lee PL, Barker FG, Louis DN, Harsh GR, Cosgrove GR, et al. In vivo 3-T MR spectroscopy in the distinction of recurrent glioma versus radiation effects: initial experience. Radiology. 2002 Dec;225(3):871–9.

127. Anbarloui MR, Ghodsi SM, Khoshnevisan A, Khadivi M, Abdollahzadeh S, Aoude A, et al. Accuracy of magnetic resonance spectroscopy in distinction between radiation necrosis and recurrence of brain tumors. Iran J Neurol. 2015 Jan 5;14(1):29–34.

128. Smith EA, Carlos RC, Junck LR, Tsien CI, Elias A, Sundgren PC. Developing a clinical decision model: MR spectroscopy to differentiate between recurrent tumor and radiation change in patients with new contrast-enhancing lesions. AJR Am J Roentgenol. 2009 Feb;192(2):W45-52.

129. Weybright P, Sundgren PC, Maly P, Hassan DG, Nan B, Rohrer S, et al. Differentiation between brain tumor recurrence and radiation injury using MR spectroscopy. AJR Am J Roentgenol. 2005 Dec;185(6):1471–6.

130. Nakajima T, Kumabe T, Kanamori M, Saito R, Tashiro M, Watanabe M, et al. Differential diagnosis between radiation necrosis and glioma progression using sequential proton magnetic resonance spectroscopy and methionine positron emission tomography. Neurol Med Chir (Tokyo). 2009 Sep;49(9):394–401.

131. Plotkin M, Eisenacher J, Bruhn H, Wurm R, Michel R, Stockhammer F, et al. 123I-IMT SPECT and 1H MR-spectroscopy at 3.0 T in the differential diagnosis of recurrent or residual gliomas: a comparative study. J Neurooncol. 2004 Oct;70(1):49–58.

132. Elias AE, Carlos RC, Smith EA, Frechtling D, George B, Maly P, et al. MR spectroscopy using normalized and non-normalized metabolite ratios for differentiating recurrent brain tumor from radiation injury. Acad Radiol. 2011 Sep;18(9):1101–8.

133. Di Costanzo A, Scarabino T, Trojsi F, Popolizio T, Bonavita S, de Cristofaro M, et al. Recurrent glioblastoma multiforme versus radiation injury: a multiparametric 3-T MR approach. Radiol Med (Torino). 2014 Aug;119(8):616–24.

134. Matsusue E, Fink JR, Rockhill JK, Ogawa T, Maravilla KR. Distinction between glioma progression and post-radiation change by combined physiologic MR imaging. Neuroradiology. 2010 Apr;52(4):297–306.

135. Prat R, Galeano I, Lucas A, Martínez JC, Martín M, Amador R, et al. Relative value of magnetic resonance spectroscopy, magnetic resonance perfusion, and 2-(18F) fluoro-2-deoxy-D-glucose positron emission tomography for detection of recurrence or grade increase in gliomas. J Clin Neurosci Off J Neurosurg Soc Australas. 2010 Jan;17(1):50–3.

136. Verma G, Chawla S, Mohan S, Wang S, Nasrallah M, Sheriff S, et al. Threedimensional echo planar spectroscopic imaging for differentiation of true progression from pseudoprogression in patients with glioblastoma. NMR Biomed. 2019;32(2):e4042.

137. Kruser TJ, Mehta MP, Robins HI. Pseudoprogression after glioma therapy: a comprehensive review. Expert Rev Neurother. 2013 Apr;13(4):389–403.

138. Law I, Albert NL, Arbizu J, Boellaard R, Drzezga A, Galldiks N, et al. Joint EANM/EANO/RANO practice guidelines/SNMMI procedure standards for imaging of gliomas using PET with radiolabelled amino acids and [18F]FDG: version 1.0. Eur J Nucl Med Mol Imaging. 2019;46(3):540–57.

139. de Zwart PL, van Dijken BRJ, Holtman GA, Stormezand GN, Dierckx RAJO, Jan van Laar P, et al. Diagnostic Accuracy of PET Tracers for the Differentiation of Tumor Progression from Treatment-Related Changes in High-Grade Glioma: A Systematic Review and Metaanalysis. J Nucl Med Off Publ Soc Nucl Med. 2020;61(4):498–504.

140. Galldiks N, Lohmann P, Albert NL, Tonn JC, Langen K-J. Current status of PET imaging in neuro-oncology. Neuro-Oncol Adv. 2019 Dec;1(1):vdz010.

141. Nandu H, Wen PY, Huang RY. Imaging in neuro-oncology. Ther Adv Neurol Disord [Internet]. 2018 Feb 28 [cited 2020 Nov 29];11. Available from:

https://www.ncbi.nlm.nih.gov/pmc/articles/PMC5833173/

142. Kertels O, Mihovilovic MI, Linsenmann T, Kessler AF, Tran-Gia J, Kircher M, et al. Clinical Utility of Different Approaches for Detection of Late Pseudoprogression in Glioblastoma With O-(2-[18F]Fluoroethyl)-L-Tyrosine PET. Clin Nucl Med. 2019 Sep;44(9):695–701.

143. Oborski MJ, Laymon CM, Lieberman FS, Mountz JM. DistinguishingPseudoprogression From Progression in High-Grade Gliomas. Clin Nucl Med [Internet]. 2013May [cited 2018 Sep 5];38(5). Available from:

https://www.ncbi.nlm.nih.gov/pmc/articles/PMC3880250/

144. Langleben DD, Segall GM. PET in differentiation of recurrent brain tumor from radiation injury. J Nucl Med Off Publ Soc Nucl Med. 2000 Nov;41(11):1861–7.

145. Horky LL, Hsiao EM, Weiss SE, Drappatz J, Gerbaudo VH. Dual phase FDG-PET imaging of brain metastases provides superior assessment of recurrence versus post-treatment necrosis. J Neurooncol. 2011 May;103(1):137–46.

146. Harat M, Małkowski B, Makarewicz R. Pre-irradiation tumour volumes defined by MRI and dual time-point FET-PET for the prediction of glioblastoma multiforme recurrence: A prospective study. Radiother Oncol J Eur Soc Ther Radiol Oncol. 2016 Aug;120(2):241–7.

147. Matuszak J, Waissi W, Clavier JB, Noël G, Namer IJ. Métastases cérébrales : apport de l'acquisition tardive en TEP/TDM au 18F-FDG pour le diagnostic différentiel entre récurrence tumorale et radionécrose. Médecine Nucl. 2016 May 1;40(3):196.

148. Padma MV, Said S, Jacobs M, Hwang DR, Dunigan K, Satter M, et al. Prediction of pathology and survival by FDG PET in gliomas. J Neurooncol. 2003 Sep;64(3):227–37.

149. Kubota R, Yamada S, Kubota K, Ishiwata K, Tamahashi N, Ido T. Intratumoral distribution of fluorine-18-fluorodeoxyglucose in vivo: high accumulation in macrophages and granulation tissues studied by microautoradiography. J Nucl Med Off Publ Soc Nucl Med. 1992 Nov;33(11):1972–80.

150. Chen W. Clinical applications of PET in brain tumors. J Nucl Med Off Publ Soc Nucl Med. 2007 Sep;48(9):1468–81.

151. Ricci PE, Karis JP, Heiserman JE, Fram EK, Bice AN, Drayer BP. Differentiating recurrent tumor from radiation necrosis: time for re-evaluation of positron emission tomography? AJNR Am J Neuroradiol. 1998 Mar;19(3):407–13.

152. Chen W, Silverman DHS, Delaloye S, Czernin J, Kamdar N, Pope W, et al. 18F-FDOPA PET imaging of brain tumors: comparison study with 18F-FDG PET and evaluation of diagnostic accuracy. J Nucl Med Off Publ Soc Nucl Med. 2006 Jun;47(6):904–11. 153. Ledezma CJ, Chen W, Sai V, Freitas B, Cloughesy T, Czernin J, et al. 18F-FDOPA PET/MRI fusion in patients with primary/recurrent gliomas: initial experience. Eur J Radiol. 2009 Aug;71(2):242–8.

154. Fueger BJ, Czernin J, Cloughesy T, Silverman DH, Geist CL, Walter MA, et al. Correlation of 6-18F-fluoro-L-dopa PET uptake with proliferation and tumor grade in newly diagnosed and recurrent gliomas. J Nucl Med Off Publ Soc Nucl Med. 2010 Oct;51(10):1532–8.

155. Herrmann K, Czernin J, Cloughesy T, Lai A, Pomykala KL, Benz MR, et al. Comparison of visual and semiquantitative analysis of 18F-FDOPA-PET/CT for recurrence detection in glioblastoma patients. Neuro-Oncol. 2014 Apr;16(4):603–9.

156. Karunanithi S, Sharma P, Kumar A, Khangembam BC, Bandopadhyaya GP, Kumar R, et al. 18F-FDOPA PET/CT for detection of recurrence in patients with glioma: prospective comparison with 18F-FDG PET/CT. Eur J Nucl Med Mol Imaging. 2013 Jul;40(7):1025–35.
157. Yu J, Zheng J, Xu W, Weng J, Gao L, Tao L, et al. Accuracy of 18F-FDOPA Positron Emission Tomography and 18F-FET Positron Emission Tomography for Differentiating Radiation Necrosis from Brain Tumor Recurrence. World Neurosurg. 2018 Jun 1;114:e1211–24.

158. Galldiks N, Dunkl V, Stoffels G, Hutterer M, Rapp M, Sabel M, et al. Diagnosis of pseudoprogression in patients with glioblastoma using O-(2-[18F]fluoroethyl)-L-tyrosine PET. Eur J Nucl Med Mol Imaging. 2015 Apr;42(5):685–95.

159. Galldiks N, Stoffels G, Filss C, Rapp M, Blau T, Tscherpel C, et al. The use of dynamic O-(2-18F-fluoroethyl)-l-tyrosine PET in the diagnosis of patients with progressive and recurrent glioma. Neuro-Oncol. 2015 Sep;17(9):1293–300.

160. Pauleit D, Floeth F, Hamacher K, Riemenschneider MJ, Reifenberger G, Müller H-W, et al. O-(2-[18F]fluoroethyl)-L-tyrosine PET combined with MRI improves the diagnostic assessment of cerebral gliomas. Brain J Neurol. 2005 Mar;128(Pt 3):678–87.

161. Kebir S, Fimmers R, Galldiks N, Schäfer N, Mack F, Schaub C, et al. Late Pseudoprogression in Glioblastoma: Diagnostic Value of Dynamic O-(2-[18F]fluoroethyl)-L-Tyrosine PET. Clin Cancer Res Off J Am Assoc Cancer Res. 2016 01;22(9):2190–6.

162. Mihovilovic MI, Kertels O, Hänscheid H, Löhr M, Monoranu C-M, Kleinlein I, et al. O-(2-(18F)fluoroethyl)-L-tyrosine PET for the differentiation of tumour recurrence from late pseudoprogression in glioblastoma. J Neurol Neurosurg Psychiatry. 2019 Feb;90(2):238–9.
163. Pöpperl G, Götz C, Rachinger W, Gildehaus F-J, Tonn J-C, Tatsch K. Value of O-(2-[18F]fluoroethyl)- L-tyrosine PET for the diagnosis of recurrent glioma. Eur J Nucl Med Mol Imaging. 2004 Nov;31(11):1464–70.

164. Mehrkens JH, Pöpperl G, Rachinger W, Herms J, Seelos K, Tatsch K, et al. The positive predictive value of O-(2-[18F]fluoroethyl)-L-tyrosine (FET) PET in the diagnosis of a glioma recurrence after multimodal treatment. J Neurooncol. 2008 May;88(1):27–35.

165. Kebir S, Khurshid Z, Gaertner FC, Essler M, Hattingen E, Fimmers R, et al. Unsupervised consensus cluster analysis of [18F]-fluoroethyl-L-tyrosine positron emission tomography identified textural features for the diagnosis of pseudoprogression in high-grade glioma. Oncotarget. 2017 Jan 31;8(5):8294–304.

166. Rachinger W, Goetz C, Pöpperl G, Gildehaus FJ, Kreth FW, Holtmannspötter M, et al. Positron emission tomography with O-(2-[18F]fluoroethyl)-l-tyrosine versus magnetic resonance imaging in the diagnosis of recurrent gliomas. Neurosurgery. 2005 Sep;57(3):505–11; discussion 505-511.

167. Werner J-M, Stoffels G, Lichtenstein T, Borggrefe J, Lohmann P, Ceccon G, et al. Differentiation of treatment-related changes from tumour progression: a direct comparison between dynamic FET PET and ADC values obtained from DWI MRI. Eur J Nucl Med Mol

Imaging. 2019 Aug;46(9):1889–901.

168. Grosu A-L, Astner ST, Riedel E, Nieder C, Wiedenmann N, Heinemann F, et al. An interindividual comparison of O-(2-[18F]fluoroethyl)-L-tyrosine (FET)- and L-[methyl-11C]methionine (MET)-PET in patients with brain gliomas and metastases. Int J Radiat Oncol Biol Phys. 2011 Nov 15;81(4):1049–58.

169. Tsuyuguchi N, Takami T, Sunada I, Iwai Y, Yamanaka K, Tanaka K, et al. Methionine positron emission tomography for differentiation of recurrent brain tumor and radiation necrosis after stereotactic radiosurgery--in malignant glioma. Ann Nucl Med. 2004 Jun;18(4):291–6.

170. De Witte O, Goldberg I, Wikler D, Rorive S, Damhaut P, Monclus M, et al. Positron emission tomography with injection of methionine as a prognostic factor in glioma. J Neurosurg. 2001 Nov;95(5):746–50.

171. Matsuo M, Miwa K, Shinoda J, Tanaka O, Krishna M. Impact of C11-methionine Positron Emission Tomography (PET) for Malignant Glioma in Radiation Therapy: Is C11methionine PET a superior to Magnetic Resonance Imaging? Int J Radiat Oncol • Biol • Phys. 2011 Oct 1;81(2):S182.

172. Matsuo M, Tanaka H, Yamaguchi T, Nishibori H, Ogawa S. Pseudoprogression of Glioblastoma Multiforme After Chemoradiation Therapy: Diagnosis by 11C-Methionine Positron Emission Tomography (PET). Int J Radiat Oncol • Biol • Phys. 2016 Oct 1;96(2):E102.

173. Tripathi M, Sharma R, Varshney R, Jaimini A, Jain J, Souza MMD, et al. Comparison of F-18 FDG and C-11 methionine PET/CT for the evaluation of recurrent primary brain tumors. Clin Nucl Med. 2012 Feb;37(2):158–63.

174. Terakawa Y, Tsuyuguchi N, Iwai Y, Yamanaka K, Higashiyama S, Takami T, et al. Diagnostic accuracy of 11C-methionine PET for differentiation of recurrent brain tumors from radiation necrosis after radiotherapy. J Nucl Med Off Publ Soc Nucl Med. 2008 May;49(5):694–9.

175. Garcia JR, Cozar M, Baquero M, Fernández Barrionuevo JM, Jaramillo A, Rubio J, et al. The value of 11C-methionine PET in the early differentiation between tumour recurrence and radionecrosis in patients treated for a high-grade glioma and indeterminate MRI. Rev Espanola Med Nucl E Imagen Mol. 2017 Apr;36(2):85–90.

176. Minamimoto R, Saginoya T, Kondo C, Tomura N, Ito K, Matsuo Y, et al. Differentiation of Brain Tumor Recurrence from Post-Radiotherapy Necrosis with 11C-Methionine PET: Visual Assessment versus Quantitative Assessment. PloS One. 2015;10(7):e0132515.

177. Li D-L, Xu Y-K, Wang Q-S, Wu H-B, Li H-S. ¹¹C-methionine and ¹⁸F-fluorodeoxyglucose positron emission tomography/CT in the evaluation of patients with suspected primary and residual/recurrent gliomas. Chin Med J (Engl). 2012 Jan;125(1):91–6.
178. Van Laere K, Ceyssens S, Van Calenbergh F, de Groot T, Menten J, Flamen P, et al. Direct comparison of 18F-FDG and 11C-methionine PET in suspected recurrence of glioma: sensitivity, inter-observer variability and prognostic value. Eur J Nucl Med Mol Imaging. 2005 Jan;32(1):39–51.

179. Dandois V, Rommel D, Renard L, Jamart J, Cosnard G. Substitution of 11C-methionine PET by perfusion MRI during the follow-up of treated high-grade gliomas: preliminary results in clinical practice. J Neuroradiol J Neuroradiol. 2010 May;37(2):89–97.
180. Deuschl C, Kirchner J, Poeppel TD, Schaarschmidt B, Kebir S, El Hindy N, et al.

11C-MET PET/MRI for detection of recurrent glioma. Eur J Nucl Med Mol Imaging. 2018;45(4):593–601.

181. Collet S, Valable S, Constans JM, Lechapt-Zalcman E, Roussel S, Delcroix N, et al. [18F]-fluoro-l-thymidine PET and advanced MRI for preoperative grading of gliomas.

NeuroImage Clin. 2015 May 29;8:448–54.

182. Chen W, Cloughesy T, Kamdar N, Satyamurthy N, Bergsneider M, Liau L, et al. Imaging proliferation in brain tumors with 18F-FLT PET: comparison with 18F-FDG. J Nucl Med Off Publ Soc Nucl Med. 2005 Jun;46(6):945–52.

183. Jacobs AH, Thomas A, Kracht LW, Li H, Dittmar C, Garlip G, et al. 18F-fluoro-Lthymidine and 11C-methylmethionine as markers of increased transport and proliferation in brain tumors. J Nucl Med Off Publ Soc Nucl Med. 2005 Dec;46(12):1948–58.

184. Ullrich R, Backes H, Li H, Kracht L, Miletic H, Kesper K, et al. Glioma proliferation as assessed by 3'-fluoro-3'-deoxy-L-thymidine positron emission tomography in patients with newly diagnosed high-grade glioma. Clin Cancer Res Off J Am Assoc Cancer Res. 2008 Apr 1;14(7):2049–55.

185. Choi SJ, Kim JS, Kim JH, Oh SJ, Lee JG, Kim CJ, et al. [18F]3'-deoxy-3'fluorothymidine PET for the diagnosis and grading of brain tumors. Eur J Nucl Med Mol Imaging. 2005 Jun;32(6):653–9.

186. Schiepers C, Dahlbom M, Chen W, Cloughesy T, Czernin J, Phelps ME, et al. Kinetics of 3'-deoxy-3'-18F-fluorothymidine during treatment monitoring of recurrent high-grade glioma. J Nucl Med Off Publ Soc Nucl Med. 2010 May;51(5):720–7.

187. Wardak M, Schiepers C, Dahlbom M, Cloughesy T, Chen W, Satyamurthy N, et al. Discriminant analysis of ¹⁸F-fluorothymidine kinetic parameters to predict survival in patients with recurrent high-grade glioma. Clin Cancer Res Off J Am Assoc Cancer Res. 2011 Oct 15;17(20):6553–62.

188. Dhermain FG, Hau P, Lanfermann H, Jacobs AH, van den Bent MJ. Advanced MRI and PET imaging for assessment of treatment response in patients with gliomas. Lancet Neurol. 2010 Sep;9(9):906–20.

189. Muzi M, Spence AM, O'Sullivan F, Mankoff DA, Wells JM, Grierson JR, et al. Kinetic analysis of 3'-deoxy-3'-18F-fluorothymidine in patients with gliomas. J Nucl Med Off Publ Soc Nucl Med. 2006 Oct;47(10):1612–21.

190. Spence AM, Muzi M, Link JM, O'Sullivan F, Eary JF, Hoffman JM, et al. NCIsponsored trial for the evaluation of safety and preliminary efficacy of 3'-deoxy-3'-[18F]fluorothymidine (FLT) as a marker of proliferation in patients with recurrent gliomas: preliminary efficacy studies. Mol Imaging Biol MIB Off Publ Acad Mol Imaging. 2009 Oct;11(5):343–55.

191. den Hollander MW, Enting RH, de Groot JC, Solouki MA, den Dunnen WFA, Sluiter WJ, et al. Prospective analysis of serial FLT-PET scanning to discriminate between true and pseudoprogression in glioblastoma. J Clin Oncol. 2014 May 20;32(15_suppl):2009–2009.

192. Brahm CG, den Hollander MW, Enting RH, de Groot JC, Solouki AM, den Dunnen WFA, et al. Serial FLT PET imaging to discriminate between true progression and pseudoprogression in patients with newly diagnosed glioblastoma: a long-term follow-up study. Eur J Nucl Med Mol Imaging. 2018 Jul 21;

193. Enslow MS, Zollinger LV, Morton KA, Kadrmas DJ, Butterfield RI, Christian PE, et al. Comparison of F-18 Fluorodeoxyglucose and F-18 Fluorothymidine Positron Emission Tomography in Differentiating Radiation Necrosis from Recurrent Glioma. Clin Nucl Med. 2012 Sep;37(9):854–61.

194. Gulyás B, Halldin C. New PET radiopharmaceuticals beyond FDG for brain tumor imaging. Q J Nucl Med Mol Imaging Off Publ Ital Assoc Nucl Med AIMN Int Assoc Radiopharmacol IAR Sect Soc Of. 2012 Apr;56(2):173–90.

195. Alkonyi B, Barger GR, Mittal S, Muzik O, Chugani DC, Bahl G, et al. Accurate differentiation of recurrent gliomas from radiation injury by kinetic analysis of α -11C-methyl-L-tryptophan PET. J Nucl Med Off Publ Soc Nucl Med. 2012 Jul;53(7):1058–64.

196. Galldiks N, Law I, Pope WB, Arbizu J, Langen K-J. The use of amino acid PET and

conventional MRI for monitoring of brain tumor therapy. NeuroImage Clin. 2017;13:386–94.
197. Barajas RF, Krohn KA, Link JM, Hawkins RA, Clarke JL, Pampaloni MH, et al.
Glioma FMISO PET/MR Imaging Concurrent with Antiangiogenic Therapy: Molecular
Imaging as a Clinical Tool in the Burgeoning Era of Personalized Medicine. Biomedicines.
2016 Oct 31;4(4).

198. Bolcaen J, Descamps B, Deblaere K, Boterberg T, De Vos Pharm F, Kalala J-P, et al. (18)F-fluoromethylcholine (FCho), (18)F-fluoroethyltyrosine (FET), and (18)F-fluorodeoxyglucose (FDG) for the discrimination between high-grade glioma and radiation necrosis in rats: a PET study. Nucl Med Biol. 2015 Jan;42(1):38–45.

199. Beshr R, Isohashi K, Watabe T, Naka S, Horitsugi G, Romanov V, et al. Preliminary feasibility study on differential diagnosis between radiation-induced cerebral necrosis and recurrent brain tumor by means of [18F]fluoro-borono-phenylalanine PET/CT. Ann Nucl Med. 2018 Dec;32(10):702–8.

200. Miyashita M, Miyatake S-I, Imahori Y, Yokoyama K, Kawabata S, Kajimoto Y, et al. Evaluation of fluoride-labeled boronophenylalanine-PET imaging for the study of radiation effects in patients with glioblastomas. J Neurooncol. 2008 Sep;89(2):239–46.

201. Zhang H, Ma L, Wu C, Xu B. Performance of SPECT in the differential diagnosis of glioma recurrence from radiation necrosis. J Clin Neurosci Off J Neurosurg Soc Australas. 2015 Feb;22(2):229–37.

202. Tie J, Gunawardana DH, Rosenthal MA. Differentiation of tumor recurrence from radiation necrosis in high-grade gliomas using 201Tl-SPECT. J Clin Neurosci Off J Neurosurg Soc Australas. 2008 Dec;15(12):1327–34.

203. Caresia AP, Castell-Conesa J, Negre M, Mestre A, Cuberas G, Mañes A, et al. Thallium-201SPECT assessment in the detection of recurrences of treated gliomas and ependymomas. Clin Transl Oncol. 2006 Oct 1;8(10):750–4.

204. Vos MJ, Tony BN, Hoekstra OS, Postma TJ, Heimans JJ, Hooft L. Systematic review of the diagnostic accuracy of 201Tl single photon emission computed tomography in the detection of recurrent glioma. Nucl Med Commun. 2007 Jun;28(6):431–9.

205. Gómez-Río M, Rodríguez-Fernández A, Ramos-Font C, López-Ramírez E, Llamas-Elvira JM. Diagnostic accuracy of 201Thallium-SPECT and 18F-FDG-PET in the clinical assessment of glioma recurrence. Eur J Nucl Med Mol Imaging. 2008 May;35(5):966–75. 206. Jeune FP –Le, Dubois F, Blond S, Steinling M. Sestamibi technetium-99m brain single-photon emission computed tomography to identify recurrent glioma in adults: 201 studies. J Neurooncol. 2006 Apr 1;77(2):177–83.

207. Palumbo B, Lupattelli M, Pelliccioli GP, Chiarini P, Moschini TO, Palumbo I, et al. Association of 99mTc-MIBI brain SPECT and proton magnetic resonance spectroscopy (1H-MRS) to assess glioma recurrence after radiotherapy. Q J Nucl Med Mol Imaging Off Publ Ital Assoc Nucl Med AIMN Int Assoc Radiopharmacol IAR Sect Soc Of. 2006 Mar;50(1):88–93.

208. Amin A, Moustafa H, Ahmed E, El-Toukhy M. Glioma residual or recurrence versus radiation necrosis: accuracy of pentavalent technetium-99m-dimercaptosuccinic acid [Tc-99m (V) DMSA] brain SPECT compared to proton magnetic resonance spectroscopy (1H-MRS): initial results. J Neurooncol. 2012 Feb;106(3):579–87.

209. Alexiou GA, Fotopoulos AD, Papadopoulos A, Kyritsis AP, Polyzoidis KS, Tsiouris S. Evaluation of brain tumor recurrence by (99m)Tc-tetrofosmin SPECT: a prospective pilot study. Ann Nucl Med. 2007 Jul;21(5):293–8.

210. Arora G, Sharma P, Sharma A, Mishra A, Hazari P, Biswas A, et al. 99mTc-Methionine Hybrid SPECT/CT for Detection of Recurrent Glioma. Clin Nucl Med [Internet].
2018 May 1 [cited 2019 May 9];43(5). Available from: insights.ovid.com

211. Santra A, Kumar R, Sharma P. Use of 99m-technetium-glucoheptonate as a tracer for

brain tumor imaging: An overview of its strengths and pitfalls. Indian J Nucl Med IJNM Off J Soc Nucl Med India. 2015;30(1):1–8.

212. Rani N, Singh B, Kumar N, Singh P, Hazari PP, Singh H, et al. Differentiation of Recurrent/Residual Glioma From Radiation Necrosis Using Semi Quantitative 99mTc MDM (Bis-Methionine-DTPA) Brain SPECT/CT and Dynamic Susceptibility Contrast-Enhanced MR Perfusion: A Comparative Study. Clin Nucl Med. 2018 Mar;43(3):e74–81.

213. Van Mieghem E, Wozniak A, Geussens Y, Menten J, De Vleeschouwer S, Van Calenbergh F, et al. Defining pseudoprogression in glioblastoma multiforme. Eur J Neurol. 2013 Oct;20(10):1335–41.

214. de Wit MCY, de Bruin HG, Eijkenboom W, Sillevis Smitt P a. E, van den Bent MJ. Immediate post-radiotherapy changes in malignant glioma can mimic tumor progression. Neurology. 2004 Aug 10;63(3):535–7.

215. Li H, Li J, Cheng G, Zhang J, Li X. IDH mutation and MGMT promoter methylation are associated with the pseudoprogression and improved prognosis of glioblastoma multiforme patients who have undergone concurrent and adjuvant temozolomide-based chemoradiotherapy. Clin Neurol Neurosurg. 2016 Dec;151:31–6.

216. Balaña C, Capellades J, Pineda E, Estival A, Puig J, Domenech S, et al. Pseudoprogression as an adverse event of glioblastoma therapy. Cancer Med. 2017 Dec;6(12):2858–66.

217. Soike MH, McTyre ER, Shah N, Puchalski RB, Holmes JA, Paulsson AK, et al. Glioblastoma radiomics: can genomic and molecular characteristics correlate with imaging response patterns? Neuroradiology. 2018 Oct;60(10):1043–51.

218. Elshafeey N, Kotrotsou A, Hassan A, Elshafei N, Hassan I, Ahmed S, et al.
Multicenter study demonstrates radiomic features derived from magnetic resonance perfusion images identify pseudoprogression in glioblastoma. Nat Commun. 2019 Jul 18;10(1):3170.
219. Ismail M, Hill V, Statsevych V, Huang R, Prasanna P, Correa R, et al. Shape Features of the Lesion Habitat to Differentiate Brain Tumor Progression from Pseudoprogression on Routine Multiparametric MRI: A Multisite Study. AJNR Am J Neuroradiol. 2018

Dec;39(12):2187–93.

220. Galldiks N, Kocher M, Langen K-J. Pseudoprogression after glioma therapy: an update. Expert Rev Neurother. 2017 Nov;17(11):1109–15.

221. Bacchi S, Zerner T, Dongas J, Asahina AT, Abou-Hamden A, Otto S, et al. Deep learning in the detection of high-grade glioma recurrence using multiple MRI sequences: A pilot study. J Clin Neurosci Off J Neurosurg Soc Australas. 2019 Dec;70:11–3.

222. Gao Y, Xiao X, Han B, Li G, Ning X, Wang D, et al. Deep Learning Methodology for Differentiating Glioma Recurrence From Radiation Necrosis Using Multimodal Magnetic Resonance Imaging: Algorithm Development and Validation. JMIR Med Inform. 2020 Nov 17;8(11):e19805.

223. Bani-Sadr A, Eker OF, Berner L-P, Ameli R, Hermier M, Barritault M, et al. Conventional MRI radiomics in patients with suspected early- or pseudo-progression. Neuro-Oncol Adv. 2019 Dec;1(1):vdz019.

224. Clark K, Vendt B, Smith K, Freymann J, Kirby J, Koppel P, et al. The Cancer Imaging Archive (TCIA): Maintaining and Operating a Public Information Repository. J Digit Imaging. 2013 Dec;26(6):1045–57.

225. Rudie JD, Rauschecker AM, Bryan RN, Davatzikos C, Mohan S. Emerging Applications of Artificial Intelligence in Neuro-Oncology. Radiology. 2019;290(3):607–18.
226. Kebir S, Schmidt T, Weber M, Lazaridis L, Galldiks N, Langen K-J, et al. A Preliminary Study on Machine Learning-Based Evaluation of Static and Dynamic FET-PET for the Detection of Pseudoprogression in Patients with IDH-Wildtype Glioblastoma. Cancers. 2020 Oct 22;12(11). 227. Artzi M, Liberman G, Nadav G, Blumenthal DT, Bokstein F, Aizenstein O, et al. Differentiation between treatment-related changes and progressive disease in patients with high grade brain tumors using support vector machine classification based on DCE MRI. J Neurooncol. 2016 May;127(3):515–24.

228. Li M, Tang H, Chan MD, Zhou X, Qian X. DC-AL GAN: Pseudoprogression and true tumor progression of glioblastoma multiform image classification based on DCGAN and AlexNet. Med Phys. 2020 Mar;47(3):1139–50.

229. Qian X, Tan H, Zhang J, Liu K, Yang T, Wang M, et al. Identification of biomarkers for pseudo and true progression of GBM based on radiogenomics study. Oncotarget. 2016 Aug 23;7(34):55377–94.

230. Jang B-S, Jeon SH, Kim IH, Kim IA. Prediction of Pseudoprogression versus Progression using Machine Learning Algorithm in Glioblastoma. Sci Rep. 2018 Aug 21;8(1):12516.

231. Lersy F, Boulouis G, Clément O, Desal H, Anxionnat R, Berge J, et al. Consensus Guidelines of the French Society of Neuroradiology (SFNR) on the use of Gadolinium-Based Contrast agents (GBCAs) and related MRI protocols in Neuroradiology. J Neuroradiol J Neuroradiol. 2020 Nov;47(6):441–9.

232. Girardi M, Kay J, Elston DM, Leboit PE, Abu-Alfa A, Cowper SE. Nephrogenic systemic fibrosis: clinicopathological definition and workup recommendations. J Am Acad Dermatol. 2011 Dec;65(6):1095-1106.e7.

233. Mathur M, Jones JR, Weinreb JC. Gadolinium Deposition and Nephrogenic Systemic Fibrosis: A Radiologist's Primer. Radiogr Rev Publ Radiol Soc N Am Inc. 2020 Feb;40(1):153–62.

234. Errante Y, Cirimele V, Mallio CA, Di Lazzaro V, Zobel BB, Quattrocchi CC. Progressive increase of T1 signal intensity of the dentate nucleus on unenhanced magnetic resonance images is associated with cumulative doses of intravenously administered gadodiamide in patients with normal renal function, suggesting dechelation. Invest Radiol. 2014 Oct;49(10):685–90.

235. Le Goff S, Barrat J-A, Chauvaud L, Paulet Y-M, Gueguen B, Ben Salem D. Compound-specific recording of gadolinium pollution in coastal waters by great scallops. Sci Rep. 2019 29;9(1):8015.

236. Schmidt K, Bau M, Merschel G, Tepe N. Anthropogenic gadolinium in tap water and in tap water-based beverages from fast-food franchises in six major cities in Germany. Sci Total Environ. 2019 Oct 15;687:1401–8.

237. Walker DT, Davenport MS, McGrath TA, McInnes MDF, Shankar T, Schieda N. Breakthrough Hypersensitivity Reactions to Gadolinium-based Contrast Agents and Strategies to Decrease Subsequent Reaction Rates: A Systematic Review and Meta-Analysis. Radiology. 2020 Aug;296(2):312–21.

238. Karsy M, Yoon N, Boettcher L, Jensen R, Shah L, MacDonald J, et al. Surgical treatment of glioblastoma in the elderly: the impact of complications. J Neurooncol. 2018 May;138(1):123–32.

239. Gulati S, Jakola AS, Nerland US, Weber C, Solheim O. The risk of getting worse: surgically acquired deficits, perioperative complications, and functional outcomes after primary resection of glioblastoma. World Neurosurg. 2011 Dec;76(6):572–9.

240. Schwartz C, Romagna A, Stefanits H, Zimmermann G, Ladisich B, Geiger P, et al. Risks and Benefits of Glioblastoma Resection in Older Adults: A Retrospective Austrian Multicenter Study. World Neurosurg. 2020 Jan;133:e583–91.

241. Dimou J, Beland B, Kelly J. Supramaximal resection: A systematic review of its safety, efficacy and feasibility in glioblastoma. J Clin Neurosci Off J Neurosurg Soc Australas. 2020 Feb;72:328–34.

242. Baron RB, Lakomkin N, Schupper AJ, Nistal D, Nael K, Price G, et al. Postoperative outcomes following glioblastoma resection using a robot-assisted digital surgical exoscope: a case series. J Neurooncol. 2020 Jul;148(3):519–27.

243. Laurent D, Freedman R, Cope L, Sacks P, Abbatematteo J, Kubilis P, et al. Impact of Extent of Resection on Incidence of Postoperative Complications in Patients With Glioblastoma. Neurosurgery. 2020 01;86(5):625–30.

244. Cebula H, Todeschi J, Le Fèvre C, Antoni D, Ollivier I, Chibbaro S, et al. [What is the place of surgery in the management of brain metastases in 2020?]. Cancer Radiother J Soc Francaise Radiother Oncol. 2020 Oct;24(6–7):470–6.

245. Rahmani R, Tomlinson SB, Santangelo G, Warren KT, Schmidt T, Walter KA, et al. Risk factors associated with early adverse outcomes following craniotomy for malignant glioma in older adults. J Geriatr Oncol. 2020 May;11(4):694–700.

246. Grossman R, Sadetzki S, Spiegelmann R, Ram Z. Haemorrhagic complications and the incidence of asymptomatic bleeding associated with stereotactic brain biopsies. Acta Neurochir (Wien). 2005 Jun;147(6):627–31; discussion 631.

247. Heper AO, Erden E, Savas A, Ceyhan K, Erden I, Akyar S, et al. An analysis of stereotactic biopsy of brain tumors and nonneoplastic lesions: a prospective clinicopathologic study. Surg Neurol. 2005;64 Suppl 2:S82-88.

248. Smith JS, Quiñones-Hinojosa A, Barbaro NM, McDermott MW. Frame-based stereotactic biopsy remains an important diagnostic tool with distinct advantages over frameless stereotactic biopsy. J Neurooncol. 2005 Jun;73(2):173–9.

249. Woodworth GF, McGirt MJ, Samdani A, Garonzik I, Olivi A, Weingart JD. Frameless image-guided stereotactic brain biopsy procedure: diagnostic yield, surgical morbidity, and comparison with the frame-based technique. J Neurosurg. 2006 Feb;104(2):233–7.

250. Dammers R, Haitsma IK, Schouten JW, Kros JM, Avezaat CJJ, Vincent AJPE. Safety and efficacy of frameless and frame-based intracranial biopsy techniques. Acta Neurochir (Wien). 2008 Jan;150(1):23–9.

251. Kongkham PN, Knifed E, Tamber MS, Bernstein M. Complications in 622 cases of frame-based stereotactic biopsy, a decreasing procedure. Can J Neurol Sci J Can Sci Neurol. 2008 Mar;35(1):79–84.

252. Chen C-C, Hsu P-W, Erich Wu T-W, Lee S-T, Chang C-N, Wei K, et al. Stereotactic brain biopsy: Single center retrospective analysis of complications. Clin Neurol Neurosurg. 2009 Dec;111(10):835–9.

253. Owen CM, Linskey ME. Frame-based stereotaxy in a frameless era: current capabilities, relative role, and the positive- and negative predictive values of blood through the needle. J Neurooncol. 2009 May;93(1):139–49.

254. Bekelis K, Radwan TA, Desai A, Roberts DW. Frameless robotically targeted stereotactic brain biopsy: feasibility, diagnostic yield, and safety. J Neurosurg. 2012 May;116(5):1002–6.

255. Lefranc M, Capel C, Pruvot AS, Fichten A, Desenclos C, Toussaint P, et al. The impact of the reference imaging modality, registration method and intraoperative flat-panel computed tomography on the accuracy of the ROSA® stereotactic robot. Stereotact Funct Neurosurg. 2014;92(4):242–50.

256. Lu Y, Yeung C, Radmanesh A, Wiemann R, Black PM, Golby AJ. Comparative effectiveness of frame-based, frameless, and intraoperative magnetic resonance imaging-guided brain biopsy techniques. World Neurosurg. 2015 Mar;83(3):261–8.

257. Nishihara M, Takeda N, Harada T, Kidoguchi K, Tatsumi S, Tanaka K, et al. Diagnostic yield and morbidity by neuronavigation-guided frameless stereotactic biopsy using magnetic resonance imaging and by frame-based computed tomography-guided stereotactic biopsy. Surg Neurol Int. 2014;5(Suppl 8):S421-426. 258. Georgiopoulos M, Ellul J, Chroni E, Constantoyannis C. Efficacy, Safety, and Duration of a Frameless Fiducial-Less Brain Biopsy versus Frame-based Stereotactic Biopsy: A Prospective Randomized Study. J Neurol Surg Part Cent Eur Neurosurg. 2018 Jan;79(1):31–8.

259. Yasin H, Hoff H-J, Blümcke I, Simon M. Experience with 102 Frameless Stereotactic Biopsies Using the neuromate Robotic Device. World Neurosurg. 2019 Mar;123:e450–6.
260. Mizobuchi Y, Nakajima K, Fujihara T, Matsuzaki K, Mure H, Nagahiro S, et al. The risk of hemorrhage in stereotactic biopsy for brain tumors. J Med Investig JMI. 2019;66(3.4):314–8.

261. Gerlinger M, Rowan AJ, Horswell S, Math M, Larkin J, Endesfelder D, et al. Intratumor Heterogeneity and Branched Evolution Revealed by Multiregion Sequencing. N Engl J Med. 2012 Mar 8;366(10):883–92.

262. Zachariah MA, Oliveira-Costa JP, Carter BS, Stott SL, Nahed BV. Blood-based biomarkers for the diagnosis and monitoring of gliomas. Neuro-Oncol. 2018 Aug 2;20(9):1155–61.

263. Klekner Á, Szivos L, Virga J, Árkosy P, Bognár L, Birkó Z, et al. Significance of liquid biopsy in glioblastoma - A review. J Biotechnol. 2019 Jun 10;298:82–7.

264. Yekula A, Muralidharan K, Rosh ZS, Youngkin AE, Kang KM, Balaj L, et al. Liquid Biopsy Strategies to Distinguish Progression from Pseudoprogression and Radiation Necrosis in Glioblastomas. Adv Biosyst. 2020 Jun 2;e2000029.

265. Sareen H, Garrett C, Lynch D, Powter B, Brungs D, Cooper A, et al. The Role of Liquid Biopsies in Detecting Molecular Tumor Biomarkers in Brain Cancer Patients. Cancers. 2020 Jul 8;12(7).

266. Smith ER, Zurakowski D, Saad A, Scott RM, Moses MA. Urinary biomarkers predict brain tumor presence and response to therapy. Clin Cancer Res Off J Am Assoc Cancer Res. 2008 Apr 15;14(8):2378–86.

267. Loo HK, Mathen P, Lee J, Camphausen K. Circulating biomarkers for high-grade glioma. Biomark Med. 2019;13(3):161–5.

268. van Schaijik B, Wickremesekera AC, Mantamadiotis T, Kaye AH, Tan ST, Stylli SS, et al. Circulating tumor stem cells and glioblastoma: A review. J Clin Neurosci Off J Neurosurg Soc Australas. 2019 Mar;61:5–9.

269. Liu T, Xu H, Huang M, Ma W, Saxena D, Lustig RA, et al. Circulating Glioma Cells Exhibit Stem Cell-like Properties. Cancer Res. 2018 Dec 1;78(23):6632–42.

270. Krol I, Castro-Giner F, Maurer M, Gkountela S, Szczerba BM, Scherrer R, et al. Detection of circulating tumour cell clusters in human glioblastoma. Br J Cancer. 2018 Aug;119(4):487–91.

271. Shankar GM, Balaj L, Stott SL, Nahed B, Carter BS. Liquid biopsy for brain tumors. Expert Rev Mol Diagn. 2017;17(10):943–7.

272. Silantyev AS, Falzone L, Libra M, Gurina OI, Kardashova KS, Nikolouzakis TK, et al. Current and Future Trends on Diagnosis and Prognosis of Glioblastoma: From Molecular Biology to Proteomics. Cells. 2019 09;8(8).

273. Müller Bark J, Kulasinghe A, Chua B, Day BW, Punyadeera C. Circulating biomarkers in patients with glioblastoma. Br J Cancer. 2020;122(3):295–305.

274. Bagley SJ, Nabavizadeh SA, Mays JJ, Till JE, Ware JB, Levy S, et al. Clinical Utility of Plasma Cell-Free DNA in Adult Patients with Newly Diagnosed Glioblastoma: A Pilot Prospective Study. Clin Cancer Res Off J Am Assoc Cancer Res. 2020 15;26(2):397–407.

275. Raza IJ, Tingate CA, Gkolia P, Romero L, Tee JW, Hunn MK. Blood Biomarkers of Glioma in Response Assessment Including Pseudoprogression and Other Treatment Effects: A Systematic Review. Front Oncol. 2020;10:1191.

276. Chistiakov DA, Chekhonin VP. Circulating tumor cells and their advances to promote

cancer metastasis and relapse, with focus on glioblastoma multiforme. Exp Mol Pathol. 2018;105(2):166–74.

277. Piccioni DE, Achrol AS, Kiedrowski LA, Banks KC, Boucher N, Barkhoudarian G, et al. Analysis of cell-free circulating tumor DNA in 419 patients with glioblastoma and other primary brain tumors. CNS Oncol. 2019;8(2):CNS34.

278. Figueroa JM, Carter BS. Detection of glioblastoma in biofluids. J Neurosurg. 2018;129(2):334–40.

279. Sullivan JP, Nahed BV, Madden MW, Oliveira SM, Springer S, Bhere D, et al. Brain tumor cells in circulation are enriched for mesenchymal gene expression. Cancer Discov. 2014 Nov;4(11):1299–309.

280. Haber DA, Velculescu VE. Blood-based analyses of cancer: circulating tumor cells and circulating tumor DNA. Cancer Discov. 2014 Jun;4(6):650–61.

281. Macarthur KM, Kao GD, Chandrasekaran S, Alonso-Basanta M, Chapman C, Lustig RA, et al. Detection of brain tumor cells in the peripheral blood by a telomerase promoterbased assay. Cancer Res. 2014 Apr 15;74(8):2152–9.

282. Müller C, Holtschmidt J, Auer M, Heitzer E, Lamszus K, Schulte A, et al. Hematogenous dissemination of glioblastoma multiforme. Sci Transl Med. 2014 Jul 30;6(247):247ra101.

283. Gao F, Cui Y, Jiang H, Sui D, Wang Y, Jiang Z, et al. Circulating tumor cell is a common property of brain glioma and promotes the monitoring system. Oncotarget. 2016 Nov 1;7(44):71330–40.

284. Shao H, Chung J, Balaj L, Charest A, Bigner DD, Carter BS, et al. Protein typing of circulating microvesicles allows real-time monitoring of glioblastoma therapy. Nat Med. 2012 Dec;18(12):1835–40.

285. Ricklefs FL, Alayo Q, Krenzlin H, Mahmoud AB, Speranza MC, Nakashima H, et al. Immune evasion mediated by PD-L1 on glioblastoma-derived extracellular vesicles. Sci Adv. 2018;4(3):eaar2766.

286. Hallal S, Ebrahimkhani S, Shivalingam B, Graeber MB, Kaufman KL, Buckland ME. The emerging clinical potential of circulating extracellular vesicles for non-invasive glioma diagnosis and disease monitoring. Brain Tumor Pathol. 2019 Apr;36(2):29–39.

287. Whitehead CA, Kaye AH, Drummond KJ, Widodo SS, Mantamadiotis T, Vella LJ, et al. Extracellular vesicles and their role in glioblastoma. Crit Rev Clin Lab Sci. 2019 Dec 22;1–26.

288. Yekula A, Minciacchi VR, Morello M, Shao H, Park Y, Zhang X, et al. Large and small extracellular vesicles released by glioma cells in vitro and in vivo. J Extracell Vesicles. 2020;9(1):1689784.

289. Naryzhny S, Volnitskiy A, Kopylov A, Zorina E, Kamyshinsky R, Bairamukov V, et al. Proteome of Glioblastoma-Derived Exosomes as a Source of Biomarkers. Biomedicines. 2020 Jul 16;8(7).

290. Hafeez U, Cher LM. Biomarkers and smart intracranial devices for the diagnosis, treatment, and monitoring of high-grade gliomas: a review of the literature and future prospects. Neuro-Oncol Adv. 2019 Dec;1(1):vdz013.

291. Hallal S, Ebrahim Khani S, Wei H, Lee MYT, Sim H-W, Sy J, et al. Deep Sequencing of Small RNAs from Neurosurgical Extracellular Vesicles Substantiates miR-486-3p as a Circulating Biomarker that Distinguishes Glioblastoma from Lower-Grade Astrocytoma Patients. Int J Mol Sci. 2020 Jul 13;21(14).

292. Koch CJ, Lustig RA, Yang X-Y, Jenkins WT, Wolf RL, Martinez-Lage M, et al.
Microvesicles as a Biomarker for Tumor Progression versus Treatment Effect in
Radiation/Temozolomide-Treated Glioblastoma Patients. Transl Oncol. 2014 Dec;7(6):752–8.
293. Osti D, Del Bene M, Rappa G, Santos M, Matafora V, Richichi C, et al. Clinical

Significance of Extracellular Vesicles in Plasma from Glioblastoma Patients. Clin Cancer Res Off J Am Assoc Cancer Res. 2019 Jan 1;25(1):266–76.

294. Zhao Z, Zhang C, Li M, Shen Y, Feng S, Liu J, et al. Applications of cerebrospinal fluid circulating tumor DNA in the diagnosis of gliomas. Jpn J Clin Oncol. 2020 Mar 9;50(3):325–32.

295. Cordova C, Syeda MM, Corless B, Wiggins JM, Patel A, Kurz SC, et al. Plasma cellfree circulating tumor DNA (ctDNA) detection in longitudinally followed glioblastoma patients using TERT promoter mutation-specific droplet digital PCR assays. J Clin Oncol. 2019 May 20;37(15_suppl):2026–2026.

296. Dong L, Li Y, Han C, Wang X, She L, Zhang H. miRNA microarray reveals specific expression in the peripheral blood of glioblastoma patients. Int J Oncol. 2014 Aug;45(2):746–56.

297. Li H-Y, Li Y-M, Li Y, Shi X-W, Chen H. Circulating microRNA-137 is a potential biomarker for human glioblastoma. Eur Rev Med Pharmacol Sci. 2016;20(17):3599–604.
298. Choppavarapu L, Kandi SM. Circulating microRNAs as Potential Biomarkers in Glioma: A Mini Review. Endocr Metab Immune Disord Drug Targets. 2020 Jul 30;

299. ParvizHamidi M, Haddad G, Ostadrahimi S, Ostadrahimi N, Sadeghi S, Fayaz S, et al. Circulating miR-26a and miR-21 as biomarkers for glioblastoma multiform. Biotechnol Appl Biochem. 2019 Mar;66(2):261–5.

300. Tabibkhooei A, Izadpanahi M, Arab A, Zare-Mirzaei A, Minaeian S, Rostami A, et al. Profiling of novel circulating microRNAs as a non-invasive biomarker in diagnosis and follow-up of high and low-grade gliomas. Clin Neurol Neurosurg. 2020;190:105652.

301. Huang S-W, Ali N, Zhong L, Shi J. MicroRNAs as biomarkers for human glioblastoma: progress and potential. Acta Pharmacol Sin. 2018 Sep;39(9):1405–13.
302. Mercatelli N, Galardi S, Ciafrè SA. MicroRNAs as Multifaceted Players in

Glioblastoma Multiforme. Int Rev Cell Mol Biol. 2017;333:269–323.

303. Morokoff A, Jones J, Nguyen H, Ma C, Lasocki A, Gaillard F, et al. Serum microRNA is a biomarker for post-operative monitoring in glioma. J Neurooncol. 2020 Sep;149(3):391–400.

304. Yin J, Zeng A, Zhang Z, Shi Z, Yan W, You Y. Exosomal transfer of miR-1238 contributes to temozolomide-resistance in glioblastoma. EBioMedicine. 2019 Apr;42:238–51.
305. Swellam M, Ezz El Arab L, Al-Posttany AS, B Said S. Clinical impact of circulating oncogenic MiRNA-221 and MiRNA-222 in glioblastoma multiform. J Neurooncol. 2019 Sep;144(3):545–51.

306. Simonelli M, Dipasquale A, Orzan F, Lorenzi E, Persico P, Navarria P, et al. Cerebrospinal fluid tumor DNA for liquid biopsy in glioma patients' management: Close to the clinic? Crit Rev Oncol Hematol. 2020 Feb;146:102879.

Table 1: Description of advanced MR	techniques metrics and resu	ilts of nseudonrogression (Psl	P) and true progression (TP)
Table 1. Description of advanced with	i comingues, men ies, and i esu	ins of pseudoprogression (1 si) and thuc progression (11).

Advanced MR	I techniques	Metrics	Results for PsP/TP
		Diffusion MRI	
DWI : Diffusion- Weighted MRI	Water diffusion within tissue (displacement of water molecules in brain parenchyma)	ADC: Apparent Diffusion Coefficient quantify the mobility of water molecules at the cellular level	ADC value: PsP>TP ADC ratio: PsP>TP
DTI : Diffusion Tensor Imaging	Direction of water diffusion	FA: Fractional Anisotropy measures the fraction of the diffusion that is anisotropic (diffusion asymmetry in a voxel)	FA value: TP>PsP FA ratio: TP>PsP
		Perfusion MRI	
DSC: Dynamic Susceptibility Contrast MRI	T2/T2*-weighted technique measurement of vascular perfusion and permeability Exogenous gadolinium based contrast agent	 rCBF: relative Cerebral Blood Flow measurement of the lesion blood flow compared to contralateral cerebral tissue (white or grey matter) rCBV: relative Cerebral Blood Volume measurement of the lesion blood volume compared to contralateral cerebral tissue (white or grey matter) PH: Peak Height reflects the total blood volume maximal signal intensity PSR: percentage of signal intensity recovery reflects capillary permeability 	rCBF: TP>PsP rCBV: TP>PsP PH: TP>PsP PSR: PsP>TP
DCE: Dynamic Contrast Enhanced	T1-based technique measurement of	K ^{trans} : Volume Transfer Constant between plasma and EES	K ^{trans} : TP>PsP

MRI	vascular parmaghility	raflacta gadalinium laakaga rata from plasma	
	vascular permeability	reflects gadolinium leakage rate from plasma to EES and microvascular permeability	
	Encorrows	to EES and microvascular permeability	
	Exogenous		
	gadolinium based	Ve: Volume of EES	V _e : TP≥PsP
	contrast agent	reflects cellularity and necrosis in EES and	
		microvascular permeability	
		V _p : Vascular plasma volume reflects blood plasma volume	V _p : TP≥PsP
		K _{ep} : Transfer constant from the EES into the plasma = Ktrans/Ve	Kep: TP=PsP
	B 1 1		
	Brain tissue	CBF: Cerebral Blood Flow	CBF : TP>PsP
	perfusion	Blood volume through a cerebral region per	
ASL: Arterial Spin		unit of time	
Labeling	Magnetic arterial		
8	blood water protons		
	as an endogenous		
	tracer		
	Magne	etic Resonance Spectroscopy	
	Reflects the	Cho: Choline	Cho/NAA: TP>PsP
MRS: Magnetic	distribution of	Cr: Creatinine	
Resonance	chemical metabolites	Lac: Lactate	Cho/Cr: TP>PsP
Spectroscopy	within a brain tissue	Lip: Lipid	
Specification	volume	NAA: N-acetylaspartate	NAA/Cr: PsP>TP

Authors	Ν	Tumors	Parameters	Val	ues	n voluo	Threshold	Se	Sp	PPV	NPV	Accuracy
Autiors	IN	Tuniors		PsP	ТР	p value	Threshold	36	Sp	FFV		Accuracy
	18	HGG	ADC ratio	1.82	1.43	<0.001						
Hein <i>et al.</i> , 2004 (67)	(8)	(GBM)	Mean ADC value	1.40	1.18	<0.006	NA	NA	NA	NA	NA	NA
			Minimal ADC value	1.04	1.07	> 0.05						
Asao et al., 2005 (64)	17 (5)	HGG (GBM)	Mean ADC value	1.68	1.37	>0.05	NA	NA	NA	NA	NA	NA
			Maximal ADC value	2.30	1.68	0.039						
Sundgren <i>et a.l</i> , 2006	28	Primary brain	Mean ADC value	1.12	1.27	0.01	NA	NA	NA	NA	NA	NA
(68)	(4)	tumor (GBM)	ADC ratio	1.40	1.54	0.07	1111	1 11 1	1111	1 11 1	1 17 1	
	55	HGG	Mean ADC value	1.39	1.20	<0.01						
Zeng et al., 2007 (74)	(19)	(GBM)	ADC ratio	1.69	1.42	<0.01	NA	NA	NA	NA	NA	NA
Bobek-Billewics et al.,	8	Gliomas	Mean ADC value	1.13	1.06	0.51	N .T. 4					27.4
2010 (81)	(2)	(GBM)	ADC ratio	1.55	1.55	0.98	NA	NA	NA	NA	NA	NA
			Mean ADC value	1.53	1.33	0.98						
Xu et al., 2010 (66)	35	Gliomas			1.20	0.0002	NA	NA	NA	NA	NA	NA
, 	(17)	(GBM)	ADC ratio	1.62	1.34	0.0013						
	20	HGG	Mean ADC value	1.349	1.040	< 0.0001						
Lee et al., 2012 (65)	22 (19)	HGG (GBM)	Mean ADC value	1.349	1.215	0.289	1.200	80	83	NA	NA	81
Fink et al., 2012 (76)	38 (10)	Gliomas (GBM)	ADC ratio	1.43	1.14	0.035	≤1.28	72	80	91	50	74
Agarwal et al., 2013 (47)	24	HGG	Mean ADC value	1.40	1.37	0.700	NA	NA	NA	NA	NA	NA

 Table 2: Review of the apparent diffusion coefficient (ADC) values in the literature for pseudoprogression (PsP) and true progression (TP).

Chu et al., 2013 (84)	30	GBM	Mean ADC value	1.329	1.269	0.616						
Alexiou et al., 2014 (78)	30 (27)	HGG (GBM)	ADC ratio	2.12	1.19	0.005	1.27	65	100	NA	NA	NA
			Median ADC lesion value	1.62	1.39	0.001						
Prager et al., 2015 (77)	68 (55)	HGG (GBM)	ADC ratio	1.585	1.482	0.288	≥1.6	95	63	NA	NA	NA
			Median ADC ROI value	1.2	1.1	0.128						
Bulik et al., 2015 (79)	24	GBM	Mean ADC value	1.373	1.160	< 0.001	1.300	100	100	NA	NA	NA
Kazda et al., 2016 (80)	39	GBM	Mean ADC value	1.372	1.155	< 0.001	1.313	98	100	NA	NA	NA
Reimer et al., 2017 (73)	35	GBM	Relative ADC			0.014	0.25	86	86	NA	NA	NA
Jena <i>et al.</i> , 2017 (75)	35 (17)	Gliomas (GBM)	Mean ADC value	1.558	1.283	0.015	≤1.507	87	55	84	58	78

ADC: Apparent diffusion coefficient; GBM: Glioblastoma; HGG: High grade gliomas; NA: not available; NPV: Negative Predictive Value; PPV: Positive Predictive Value; PsP: Pseudoprogression; ROI: Region of interest; TP: True Progression; Se: Sensibility; Sp: Specificity

A with our	NI	Tumona	Devenuetors	Va	lues		Threaded	Se	S m	PPV	NPV	
Authors	Ν	Tumors	Parameters	PsP	ТР	р	Threshold	Se	Sp	PPV	NPV	Accuracy
			Mean rCBV	1.57	2.38	<0.01	1.75	79	72			
			Max rCBV	4.63	8.16	<0.01						
			Min rCBV	0.95	1.61	<0.01						
			Mean rPH	1.25	2.7	<0.01	1.38	89	81			
Barajas <i>et al.</i> , 2009 (122)	57	GBM	Max rPH	1.72	3.09	<0.01				NA	NA	NA
			Min rPH	0.82	1.31	<0.01						
			Mean rPSR	89.3	80.2	0.01	87.3	78	76			
			Max rPSR	92.5	100	0.05						
			Min rPSR	77.2	68.8	0.04						
	13	HGG	Min rCBV	0.21	0.55		0.71	92	100			96
Hu et al., 2009 (95)	(9)	(GBM)	Max rCBV	0.71	4.64					NA	NA	
Gasparetto <i>et al.</i> , 2009 (97)	12	GBM	Mean rCBV				1.8	100	87	80	100	92
Bobek-Billewics <i>et al.</i> ,	8	Gliomas	Max rCBV	0.78	2.44	<0.001	≥1.7					
2010 (81)	(2)	(GBM)	Mean rCBV	0.49	1.46	<0.004	≥1.25	NA	NA	NA	NA	NA
Tsien et al., 2010 (104)	27 (23)	HGG (GBM)	Mean rCBV	2.3	2.8	0.8	NA	NA	NA	NA	NA	NA
Kim et al., 2010 (99)	10	HGG	Mean rCBV	2.53	5.72	0.01	3.69	100	100	NA	NA	NA

Table 3: Review of the perfusion MRI metrics in the literature and their statistical characteristics

	(5)	(GBM)										
Heidemans-Hazelaar et al., 2010 (94)	32	GBM	Mean rCBV			<0.002	2.12	88	83	96	63	NA
			Median K ^{trans}	0.15	0.43	0.0051	>0.19	100	83			
Bisdas et al., 2011 (110)	18	HGG	Median V _e	0.34	0.56	NS				NA	NA	NA
			Median Kep	0.34	0.45	NS						
Gahramanov <i>et al.</i> , 2011 (98)	14	GBM	Mean rCBV	0.7	2.7	NA	1.75	NA	NA	NA	NA	NA
Kong et al., 2011 (107)	59	GBM	Mean rCBV	1.49	2.85	0.003	>1.49	81	78	NA	NA	NA
Fink et al., 2012 (76)	38 (10)	Gliomas (GBM)	CBV ratio	1.31	3.62	<0.001	≥2.08	86	90	96	69	87
Hu et al., 2012 (96)	25	GBM	Mean rCBV				1.0	100	100	NA	NA	100
Young <i>et al.</i> , 2013 (100)	20	GBM	Median rCBV Mean rPH	1.50 1.34	2.75 3.04	0.009 <0.001	≤1.8 ≤2.4 ≤1.7	100 69 100	75 100 100	NA	NA	NA
			Mean PSR	1.01	0.84	<0.039	≥0.9	100	63			
Larsen <i>et al.</i> , 2013 (28)	19 (13)	Gliomas (GBM)	Mean CBV Mean CBF	1.3 11.9	10.9 28.1	NA NA	2.0	100	100	NA	NA	NA
			Mean rCBF (DSC)	1.66	4.01	<0.01	2.24	77	85			80
			Mean rCBF (ASL)	1.66	2.41	0.063	2.18	54	85			69
Seeger et al., 2013 (92)	40	HGG	Mean rCBV	1.73	3.91	0.01	2.15	81	77	NA	NA	79
			Median K ^{trans}	0.03	0.05	0.07	>0.058	62	80			69
			Maximum K ^{trans}	0.047	0.08	0.046						

			Ve	0.15	0.27	0.10						
Alexiou <i>et al.</i> , 2014 (78)	30 (27)	HGG (GBM)	Mean rCBV	1.68	6.71	0.000	2.2	100	100	NA	NA	NA
D'Souza et al., 2014 (93)	29 (13)	HGG (GBM)	Mean rCBV	3.01	0.8	NA	NA	NA	NA	NA	NA	NA
Shin et al., 2014 (105)	31 (18)	Gliomas (GBM)	Mean rCBV	2.11	2.55	0.511	2.33	72	70	NA	NA	NA
			Mean rK ^{trans} Mean K ^{trans}	1.69 0.23	2.52 0.44	0.399 0.004	2.1 0.347	61 59	80 94	91	68	76
Yun et al., 2015 (111)	33	GBM	Ve	0.75	1.26	0.034	0.570	88	56	68	82	
			V_p	0.11	0.14	0.119						
			Mean V _p	2.4	5.3	0.0002	>3.7	85	79			
Thomas <i>et al.</i> , 2015	37	CDM	90 th percentile V _p	3.2	6.6	>0.0001	>3.9	85	92	NT A	NTA	NT A
(112)	57	GBM	Mean K ^{trans}	3.5	7.4	0.002	>3.6	69	79	NA	NA	NA
			90 th percentile K ^{trans}	4.2	9.1	0.0004						
			Median rCBVlesion	0.88	1.76	0.028	<1.07	75	100			
Prager <i>et al.</i> , 2015 (77)	68 (55)	HGG (GBM)	Median rCBVroi	1.625	2.575	0.032	<1.74	75	93	NA	NA	NA
			Median rPSRroi	0.87	0.80	0.467						
Wang et al., 2016 (85)	41	GBM	Max rCBV	2.90	4.75	0.007	4.06	62	80	NA	NA	NA
Jena et al., 2017 (75)	35 (17)	Gliomas (GBM)	Mean rCBV	1.82	2.41	0.082	≥1.71	NA	NA	NA	NA	77
Boxerman <i>et al.</i> , 2017 (103)	9 (6)	HGG (GBM)	Mean rCBV	2.4	2.2	0.67	>2.4	67	40	NA	NA	NA

GBM: Glioblastoma; **HGG**: High Grade Glioma; **K**_{ep}: Transfer constant from the extracellular-extravascular space into the plasma; **K**^{trans}: Volume Transfer Constant; **NA**: not available; **NPV**: Negative Predictive Value; **PPV**: Positive Predictive Value; **PsP**: Pseudoprogression; **rCBF**: relative Cerebral Blood Flow; **rCBV**: relative Cerebral Blood Volume; **ROI**: Regio of Interest; **rPH**: relative Peak Height; **rPSR**: relative Percentage of Signal intensity Recovery; **TP**: True Progression; **Se**: Sensibility; **Sp**: Specificity; **V**_e: Volume of extravascular-extracellular space; **V**_p: Vascular plasma volume

Parameters	Authors	Ν	Tumors	Va	lues	n	Threshold	Se	Sp	PPV	NPV	
Parameters	Authors		1 uniors	PsP	TP	р	Threshold	Se	Sp	FFV		Accuracy
	Plotkin et al., 2004 (131)	25	Gliomas	0.74	1.51	<0.0001	1.17	89	83	NA	NA	88
		(10)	(GBM)									
	Weybright <i>et al.</i> , 2005 (129)	29	Primary	1.31	3.48	<0.0001	1.8	NA	NA	NA	NA	NA
			brain									
			tumors									
	Zeng et al., 2007 (74)	55	HGG	1.55	3.52	<0.01	NA	NA	NA	NA	NA	NA
		(19)	(GBM)									
	Smith <i>et al.</i> , 2009 (128)	33 (4)	Primary	1.43	3.20	0.0007	NA	85	69	81	NA	NA
			brain									
			tumors									
		0 (2)	(GBM)	0.11	1.0	0.51	NT A	N T 4	NT A	NT 4	NT 4	
	Bobek-Billewicz et al., 2010 (81)	8 (2)	Gliomas	2.11	1.9	0.51	NA	NA	NA	NA	NA	NA
Cho/NAA	$E_{1,2,2} = (-1, -2, 0, 1, 1, 1, 2, 2)$	25(2)	(GBM)	1 20	2.01	0.0004	NA	NT A	NA	NA	NA	NA
CIIO/INAA	Elias <i>et al.</i> , 2011 (132)	25 (2)	Primary brain	1.39	2.81	0.0004	INA	NA	INA	INA	INA	INA
			tumors									
			(GBM)									
	Fink <i>et al.</i> , 2012 (76)	38	Gliomas	0.84	2.87	0.002	NA	NA	NA	NA	NA	NA
	T hik et ut., 2012 (70)	(10)	(GBM)	0.01	2.07	0.002	1 17 1	1111	1111	1 1 1	1111	1 11 1
	Seeger et al., 2013 (92)	40	HGG	1.47	2.20	0.20	NA	NA	NA	NA	NA	NA
	Anbarloui et al., 2015 (127)	33	Primary	1.46	2.72	<0.01	>1.8	84	75	NA	NA	81
		(13)	brain									
			tumors									
			(GBM)									
	Bulik et al., 2015 (79)	24	GBM	0.77	2.00	<0.001	≥1.4	100	92	NA	NA	NA

Table 4: Review of the different publications regarding MRS and the reported threshold values, sensitivity (Se), specificity (Sp), positive predictive value (PPV), negative predictive value (NPV), and accuracy

	Kazda <i>et al.</i> , 2016 (80)	39	GBM	0.74	2.13	<0.001		100	95	NA	NA	NA
							≥1.3					
	Plotkin <i>et al.</i> , 2004 (131)	25	Gliomas	0.95	1.38	0.030	1.11	89	83	NA	NA	88
		(10)	(GBM)	1 55	0.50	.0.0001	1.0					
	Weybright <i>et al.</i> , 2005 (129)	29	Primary brain	1.57	2.52	<0.0001	1.8	NA	NA	NA	NA	NA
			tumors									
	Zeng et al., 2007 (74)	55	HGG	1.61	2.82	<0.01	2.5	78	86	NA	NA	NA
		(19)	(GBM)									
	Nakajima <i>et al.</i> , 2009 (130)	18 (8)	Gliomas	2.25	3.17	NS	NA	NA	NA	NA	NA	NA
	Smith at al. $2000(128)$	33 (4)	(GBM)	1.57	2.36	0.0001	NA	NA	NA	NA	NA	NA
	Smith <i>et al.</i> , 2009 (128)	33 (4)	Primary brain	1.37	2.30	0.0001	INA	INA	INA	ΝA	INA	NA
			tumors									
			(GBM)									
	Bobek-Billewicz et al., 2010 (81)	8 (2)	Gliomas	1.84	2.23	0.2441	NA	NA	NA	NA	NA	NA
Cho/Cr	Elice et al. $2011(122)$	25(2)	(GBM)	1.34	2.16	0.15	NA	NA	NA	NA	NA	NA
	Elias <i>et al.</i> , 2011 (132)	25 (2)	Primary brain	1.54	2.10	0.15	INA	INA	ΝA	ΝA	INA	INA
			tumors									
			(GBM)									
	Fink <i>et al.</i> , 2012 (76)	38	Gliomas	1.57	2.57	0.021	NA	NA	NA	NA	NA	NA
	Seeger <i>et al.</i> , 2013 (92)	(10) 40	(GBM) HGG	1.30	1.66	0.047	>1.12	85	50	NA	NA	72
	Seeger <i>et ut.</i> , 2013 (92)	40	1100	1.50	1.00	0.047	/1.12	05	50	INA	INA	12
	D'Souza <i>et al.</i> , 2014 (93)	29	HGG	1.26	2.27	NA	≥0.7	83	42	NA	NA	NA
		(13)	(GBM)									
	Bulik <i>et al.</i> , 2015 (79)	24	GBM	0.82	0.86	0.317	≥1.405	NA	NA	NA	NA	91
	Jena <i>et al.</i> , 2017 (75)	35	Gliomas	1.63	3.47	0.002	>0.7	75	63	NA	NA	NA
	Jena et al., 2017 (75)	(17)	(GBM)	1.05	5.47	0.002	≥0.7	15	05	INA	INA	
	Kazda <i>et al.</i> , 2016 (80)	39	GBM	0.64	0.89	0.013	NA	NA	NA	NA	NA	NA

	Plotkin et al., 2004 (131)	25	Gliomas	1.44	0.99	0.212	NA	NA	NA	NA	NA	NA
		(10)	(GBM)									
	Weybright <i>et al.</i> , 2005 (129)	29	Primary	1.22	0.79	<0.0001	NA	NA	NA	NA	NA	NA
			brain									
			tumors									
	Zeng et al., 2007 (74)	55	HGG	1.10	0.84	<0.01	NA	NA	NA	NA	NA	NA
		(19)	(GBM)									
	Smith <i>et al.</i> , 2009 (128)	33 (4)	Primary	1.14	0.85	0.0183	NA	NA	NA	NA	NA	NA
			brain									
NAA/Cr			tumors									
		25(2)	(GBM)	1.20	0.05	0.0022	NT A					
	Elias <i>et al.</i> , 2011 (132)	25 (2)	Primary	1.36	0.85	0.0033	NA	NA	NA	NA	NA	NA
			brain									
			tumors (GBM)									
	Seeger <i>et al.</i> , 2013 (92)	40	HGG	0.51	1.01	0.051	NA	NA	NA	NA	NA	NA
	Seeger <i>et ul.</i> , 2015 (92)	40	1100	0.51	1.01	0.031	INA	INA	INA	INA	INA	INA
	Bulik <i>et al.</i> , 2015 (79)	24	GBM	0.99	0.45	< 0.001	≤0.7	94	92	NA	NA	NA
	Buik et ut., 2015 (77)	21	ODM	0.77	0.15	10.001	_0.7		12	1111	1111	1 1 1
	Kazda et al., 2016 (80)	39	GBM	0.99	0.41	<0.001	≤0.7	97	95	NA	NA	NA
	Anbarloui et al., 2015 (127)	33	Primary	0.6	2.78	<0.01	>1.0	84	75	NA	NA	81
Cho/Lip		(13)	brain									
Clio/Lip			tumors									
			(GBM)									
Lac/Cr	Zeng et al., 2007 (74)	55	HGG	0.45	1.28	0.01	NA	NA	NA	NA	NA	NA
		(19)	(GBM)									
Lip/Cr	Zeng et al., 2007 (74)	55	HGG	0.54	0.14	0.01	NA	NA	NA	NA	NA	NA
Lip, Ci		(19)	(GBM)									
Lac/Cho	Nakajima <i>et al.</i> , 2009 (130)	18 (8)	Gliomas	2.35	0.63	<0.01	1.05	89	100	NA	NA	NA
Lucient			(GBM)									
(Lac+Lip)/Cr	Bulik <i>et al.</i> , 2015 (79)	24	GBM	0.88	4.43	0.004	≥1.9	92	75	NA	NA	NA

	Kazda <i>et al.</i> , 2016 (80)	39	GBM	1.13	2.69	0.005	≥1.6	76	68	NA	NA	NA
Lac+Lip	Bulik et al., 2015 (79)	24	GBM	3.50	10.77	0.004	≥4.8	100	67	NA	NA	NA
Cho	Bulik et al., 2015 (79)	24	GBM	2.88	2.41	0.739	≤2.9	69	42	NA	NA	NA
NAA	Bulik et al., 2015 (79)	24	GBM	2.88	1.19	<0.001	≤1.5	75	100	NA	NA	NA
Cr	Bulik <i>et al.</i> , 2015 (79)	24	GBM	2.74	2.49	0.243	≤2.6	56	67	NA	NA	NA

Cho:Choline; **Cr**:Creatinine; **Lac**:Lactates; **Lip**:Lipids; **NAA**:N-acetylaspartate; **NPV**: Negative Predictive Value; **PPV**: Positive Predictive Value; **PsP**: Pseudoprogression; **TP**: True Progression; **Se**: Sensibility; **Sp**: Specificity

Table 5: Different tracers and	metrics of positron-em	ission tomography (PET).

PET tracers		Metrics	TP/PsP
FDG	2-deoxy-2-[fluorine-18]fluoro- D-glucose		
FDOPA	¹⁸ F-fluoro-L-dopa	SUV: standardized uptake value	TP>PsP
FET	O-(2-[¹⁸ F]fluoroethyl)-L-tyrosine	T/N: tumor uptake to normal hemispheric tissue uptake	TP>PsP
MET	¹¹ C-methyl-L-methionine	T/S: tumor uptake to striatum uptake	TP>PsP
FLT	3'-deoxy-3'[(18)F]-fluorothymidine	L/N: lesion uptake to normal brain tissue uptake	TP>PsP
Choline	¹¹ C-Choline	L/R: lesion uptake to contralateral cerebral white matter uptake TBR: tumor-to-brain ratio	TP>PsP TP>PsP
FMISO	¹⁸ F-Fluoromisonidazole	TNR: tumor-to-normal brain ratio	TP>PsP
MLT	¹¹ C-Methyl-L-Tryptophan PET	SUV/BG: standardized uptake value/background	TP>PsP
FCho	¹⁸ F-fluoromethylcholine	TTP: time to peak	PsP>TP
FBPA	4-borono-2- ¹⁸ F-fluoro-phenylalanine		1 51 / 11

PET: Positrion Emisson Tomography; **PsP:** Pseudoprogression; **TP**: True Progression

 Table 6: Comparison of single imaging techniques to differentiate PsP versus TP according to the literature review.

Imaging technique		Features	Sensitivity	Specificity	Accuracy
Conventional MRI		High availabilityLow time acquisitionStandardized protocol acquisition and recommendations (BPTI)More research and larger studiesLimited sensitivity, specificity and accuracyImpact of treatment use (corticosteroids, antiangiogenics)	68-83%	25-77%	67%
Advanced MRI	Diffusion MRI	High availability Lack of standardized protocol Leakage correction needed	65-100%	55-100%	74-86%
	Perfusion MRI	Lower resolution Impact of treatment use (corticosteroids, antiangiogenics)	54-100%	40-100%	69-100%
MRS		High availability (monovoxel>multivoxel) Higher specificity and accuracy (monovoxel>multivoxel) Lower spatial resolution (monovoxel>multivoxel) Lack of reproducibly and variability (multivoxel>monovoxel) Long acquisition time (multivoxel>monovoxel) Long processing time (multivoxel>monovoxel) Long interpretation time (multivoxel>monovoxel) Lack of standardized threshold and various metabolic ratios (multivoxel>monovoxel) Signal contamination (lipids, water) (multivoxel>monovoxel) Impact of treatment use (corticosteroids, antiangiogenics), measurable	75-100%	40-95%	72-93%
PET	FDG	Standardized protocols and guidelines Higher sensitivity and accuracy	46-86%	22-100%	57-63%
	FDOPA	Variable availability Variable cerebral activity	84-100%	43-100%	78-96%

	FET	Variable half-life Variable stability	68-100%	70-100%	71-96%
	MET	Poor resolution	75-100%	60-100%	75-94%
					Need
	FLT		91-100%	0-100%	additional
				researches	
	FMISO		Need	Need	Need
			additional	additional	additional
			researches	researches	researches
BPTI: International Brain Tumor Imaging; FDG: Fluoro-Deoxy-Glucose; FDOPA: Fluoro-L-Dopa; FET: Fluoroethyl-L-Tyrosine; FLT: F-					
Fluorothymidine; FMISO: F-fluoromisonidazole; MET: methyl-L-methionine; MRI: Magnetic Resonance Imaging; MRS: Magnetic					

Positron

Emission

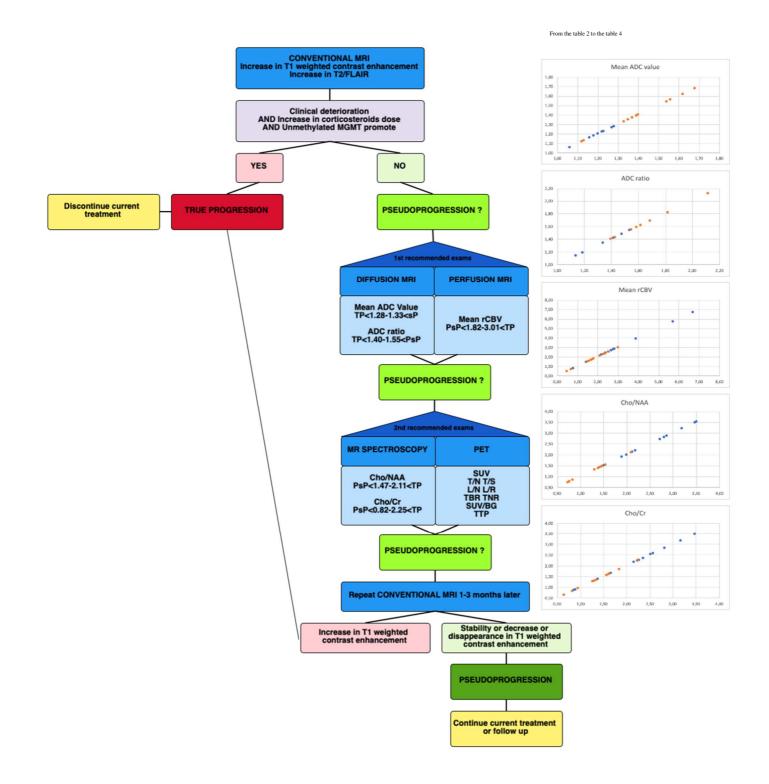
PET:

Spectroscopy;

Resonance

Tomography

Figure 1: Clinical decisional diagram between pseudoprogression (PsP) and true progression (TP)



69